A high order mixed-FEM for diffusion problems on curved domains*

Ricardo Oyarzúa[†] Manuel Solano[‡] Paulo Zúñiga[§]

June 1, 2018

Abstract

We propose and analyze a high order mixed finite element method for diffusion problems with Dirichlet boundary condition on a domain Ω with curved boundary Γ. The method is based on approximating Ω by a polygonal subdomain D_h, with boundary Γ_h, where a high order conforming Galerkin method is considered to compute the solution. To approximate the Dirichlet data on the computational boundary Γ_h, we employ a transferring technique based on integrating the extrapolated discrete gradient along segments joining Γ_h and Γ. Considering general finite dimensional subspaces we prove that the resulting Galerkin scheme, which is $\mathbf{H}(\mathrm{div}\,;\mathrm{D}_h)$-conforming, is well-posed provided suitable hypotheses on the aforementioned subspaces and integration segments. A feasible choice of discrete spaces is given by Raviart–Thomas elements of order $k \geq 0$ for the vectorial variable and discontinuous polynomials of degree k for the scalar variable, yielding optimal convergence if the distance between Γ_h and Γ is at most of the order of the meshsize h. We also approximate the solution in $\mathrm{D}_h^c := \Omega \backslash \overline{\mathrm{D}_h}$ and derive the corresponding error estimates. Numerical experiments illustrate the performance of the scheme and validate the theory.

Key words: curved domain, high order, diffusion problem, mixed variational formulation

Mathematics subject classifications (2010): 65N30, 65N12, 65N15

1 Introduction

This work proposes and analyzes a high order mixed finite element method applied to a diffusion problem with Dirichlet boundary conditions on a domain Ω not necessarily polygonal. More precisely, given $f \in \mathrm{L}^2(\Omega)$ and $g \in \mathrm{H}^{1/2}(\Gamma)$ we are interested in approximating, by a mixed finite element discretization, the vector field $\boldsymbol{\sigma}$ and the scalar field u satisfying the following first–order system of equations

$$\boldsymbol{\sigma} = \nabla u \quad \text{in} \quad \Omega, \quad \mathrm{div}\,\boldsymbol{\sigma} = -f \quad \text{in} \quad \Omega, \quad u = g \quad \text{on} \quad \Gamma, \tag{1.1}$$

*R. Oyarzúa acknowledges partial support from CONICYT-Chile through project Fondecyt 1161325 and project AFB170001 of the PIA Program: Concurso Apoyo a Centros Científicos y Tecnológicos de Excelencia con Financiamiento Basal and from Universidad del Bío-Bío through DIUBB project GI 171508/VC. M. Solano acknowledges partial support from CONICYT-Chile through project Fondecyt 1160320 and project AFB170001 of the PIA Program: Concurso Apoyo a Centros Científicos y Tecnológicos de Excelencia con Financiamiento Basal. P. Zúñiga acknowledges Becas-Chile Program.

[†]GIMNAP-Departamento de Matemática, Universidad del Bío-Bío, Casilla 5-C, Concepción, Chile, and CI^{2}MA, Universidad de Concepción, Casilla 160-C, Concepción, Chile, email: `royarzua@ubiobio.cl`.

[‡]CI^{2}MA and Departamento de Ingeniería Matemática, Universidad de Concepción, Casilla 160-C, Concepción, Chile email: `msolano@ing-mat.udec.cl`.

[§]CI^{2}MA and Departamento de Ingeniería Matemática, Universidad de Concepción, Casilla 160-C, Concepción, Chile, email: `pzuniga@ci2ma.udec.cl`.

where $\Gamma := \partial\Omega$ is the boundary of Ω, which is assumed to be piecewise $\mathcal{C}^2$ and Lipschitz. Our approach is based on a technique originally developed in the context of high order hybridizable discontinuous Galerkin (HDG) methods [13, 15, 17]. It consists of approximating Ω by a polygonal subdomain D_h, with boundary Γ_h, and transferring the Dirichlet boundary datum g from Γ to the computational boundary Γ_h, in such a way that the method keeps high order accuracy when D_h does not necessarily fit Ω. As we will detail below in Section 2.1, the transferred boundary datum on Γ_h, denoted by $\widetilde{g}$, is obtained by integrating $\boldsymbol{\sigma} = \nabla u$ along a family of segments joining Γ_h and Γ, which will be referred as *transferring paths*. At discrete level, $\widetilde{g}$ is approximated by a boundary datum $\widetilde{g}_h$ obtained by integrating the extrapolation of the discrete approximation of $\boldsymbol{\sigma}$ along the transferring paths. Thus, the problem is solved in D_h by means of any standard mixed method for polygonal domains.

This technique, as mentioned before, has been introduced for HDG methods. It was first proposed and analyzed for the one-dimensional case in [13]. The approach was extended in [15] to two dimensions where numerical evidence indicated that the method performs optimally. Later, the authors in [17] proved that the method converges with optimal order in two and three dimensions under assumptions regarding the transferring paths. In addition, this technique has been successfully applied to convection-diffusion problems [16], exterior diffusion equations [14] and the Stokes flow problem [31]. We point out that in all these work the distance $d(\Gamma_h, \Gamma)$ between Γ_h and Γ is only of the order of the meshize h and there is no need of fitting the domain Ω. On the other hand, also in the context of HDG methods, [29] applied this technique to a diffusion problem with mixed boundary conditions and to an elliptic transmission problem where the interface is not piecewise flat. In these two cases, the boundary/interface needs to be interpolated by a piecewise linear computational boundary/interface in order to obtain high order accuracy, which means that the distance between the computational boundary/interface and the true boundary/interface has to be at most of order h^2. The reason why this approach works for the Dirichlet problem under less restrictive assumption than the Neumann problem ($d(\Gamma_h, \Gamma)$ of order h versus order h^2) relies on the fact that the PDE provides a way to determine the Dirichlet data at the computational boundary through performing a line integration of the equation $\boldsymbol{\sigma} = \nabla u$. An appropriate transferring procedure of the Neumann datum, allowing $d(\Gamma_h, \Gamma)$ to be of order h, remains as an open problem.

On the other hand, a variety of numerical methods dealing with curved boundaries or interfaces have been proposed since the seventies, most of them provide low order approximations. In general, they can be classified in two groups: *fitted* and *unfitted* methods. *Fitted* methods fit the computational boundary to Γ. For example, Γ_h can be constructed by a linear interpolation of Γ and the boundary data is transferred in a *natural way*, i.e., if $x \in \Gamma_h$ and $\bar{x} \in \Gamma$ is a projection of x in Γ, then $\widetilde{g}(x) := g(\bar{x})$. We recall that $\widetilde{g}$ denotes the boundary data on Γ_h. This idea, which was first introduced in [4] and then extended to interface problems in [5], leads to a low order approximation. To achieve a high order approximation in the context of fitted methods, an alternative procedure is to use isoparametric finite elements (see e.g. [25]). However, these meshes are not easy to construct, especially for complicated geometries or when dealing with moving domains. On the contrary, *unfitted* methods, such as the immersed boundary method, allow us to work with background meshes, which is useful in complicated geometries. Nevertheless, since the boundary of the resulting polygonal domain is "far" from the curved boundary, the boundary data must be incorporated differently from the classical approaches. We refer the reader to [17, Section 1] for a review of *unfitted* methods, including the work [3, 26, 27, 28].

The method presented in this manuscript can be classified as an *unfitted* method, where the boundary data is transferred in such a way that optimal high order accuracy is achieved. To the best of our knowledge, this technique has only been applied to HDG methods. Therefore, the purpose of our work is to consider this approach to the context of dual–mixed formulations of elliptic problems. The literature regarding mixed methods in polygonal/polyhedral domains is extensive. For instance we refer the reader to [9] and [21] for a detailed analysis of mixed methods applied to different problems. However, in the context of curved domains the literature is scarce. Up to the author's knowledge, probably the only work dealing with mixed methods in curved domains are [7, 8], where a parametric Raviart–Thomas finite elements for domains with curved boundaries is employed.

The rest of this work is organized as follows. In the remainder of this section we recall notation and general definitions. Then, the domain Ω is approximated by a polygonal subdomain where a Galerkin scheme is introduced and analyzed in Section 2. In Section 3, we derive the corresponding *a priori* error analysis whenever the distance $\mathrm{d}(\Gamma, \Gamma_h)$ is at most $\mathcal{O}(h)$. Next, in Section 4 we make precise the definition of the involved discrete spaces, recall some approximation properties, and Finally, conclusions are drawn in Section 6.

We end this section by introducing definitions and notations. In the sequel, when no confusion arises, $|\cdot|$ will denote the Euclidean norm in $\mathbb{R}^2$. Additionally, in what follows we utilize standard simplified terminology for Sobolev spaces and norms, where spaces of vector-valued functions are denoted in bold face. In particular, if $\mathcal{O}$ is a domain in $\mathbb{R}^2$, Σ is an open or closed Lipschitz curve, and $s \in \mathbb{R}$, we define

$$\mathbf{H}^s(\mathcal{O}) := [\mathrm{H}^s(\mathcal{O})]^2 \quad \text{and} \quad \mathbf{H}^s(\Sigma) := [\mathrm{H}^s(\Sigma)]^2.$$

However, when $s = 0$ we write $\mathbf{L}^2(\mathcal{O})$ and $\mathbf{L}^2(\Sigma)$ instead of $\mathbf{H}^0(\mathcal{O})$ and $\mathbf{H}^0(\Sigma)$, respectively. The corresponding norms are denoted by $\|\cdot\|_{s,\mathcal{O}}$ for $\mathrm{H}^s(\mathcal{O})$, $\mathbf{H}^s(\mathcal{O})$, and $\|\cdot\|_{s,\Sigma}$ for $\mathrm{H}^s(\Sigma)$ and $\mathbf{H}^s(\Sigma)$. For $s \geq 0$, we write $|\cdot|_{s,\mathcal{O}}$ for the $\mathbf{H}^s$-seminorm and H^s-seminorm. In addition, we define the Sobolev space (see, e.g. [9, 21, 23]):

$$\mathbf{H}(\mathrm{div}\,; \mathcal{O}) := \left\{ \boldsymbol{\tau} := (\tau_1, \tau_2)^{\mathrm{t}} \in \mathbf{L}^2(\mathcal{O}) : \ \mathrm{div}\, \boldsymbol{\tau} \in \mathrm{L}^2(\mathcal{O}) \right\},$$

equipped with the norm $\|\boldsymbol{\tau}\|_{\mathrm{div}\,;\mathcal{O}} := \left(\|\boldsymbol{\tau}\|_{0,\mathcal{O}}^2 + \|\mathrm{div}\, \boldsymbol{\tau}\|_{0,\mathcal{O}}^2 \right)^{1/2}$, where the divergence operator div is understood in the sense of distributions, that is,

$$\langle \mathrm{div}\, \boldsymbol{\tau}, \varphi \rangle_{\mathscr{D}'(\mathcal{O}) \times \mathscr{D}(\mathcal{O})} := -\int_{\mathcal{O}} \boldsymbol{\tau} \cdot \nabla \varphi \, d\mathbf{x} \quad \forall\, \varphi \in \mathscr{D}(\mathcal{O}) := \mathcal{C}_0^\infty(\mathcal{O}),$$

with $\langle \cdot, \cdot \rangle_{\mathscr{D}'(\mathcal{O}) \times \mathscr{D}(\mathcal{O})}$ being the distributional paring between $\mathscr{D}'(\mathcal{O})$ and $\mathscr{D}(\mathcal{O})$. Note that if $\boldsymbol{\tau} \in \mathbf{H}(\mathrm{div}\,; \mathcal{O})$, then $\boldsymbol{\tau} \cdot \boldsymbol{\nu}_{\partial\mathcal{O}} \in \mathrm{H}^{-1/2}(\partial\mathcal{O})$, where $\boldsymbol{\nu}_{\partial\mathcal{O}}$ denotes the outward unit vector normal to the boundary $\partial\mathcal{O}$ and $\mathrm{H}^{-1/2}(\partial\mathcal{O})$ corresponds to the dual space of $\mathrm{H}^{1/2}(\mathcal{O})$. Hereafter, $\langle \cdot, \cdot \rangle_{\partial\mathcal{O}}$ denotes the duality pairing between $\mathrm{H}^{-1/2}(\partial\mathcal{O})$ and $\mathrm{H}^{1/2}(\partial\mathcal{O})$ with respect to the $\mathrm{L}^2(\partial\mathcal{O})$-inner product.

Finally, by $\mathbf{0}$ we will refer to the generic null vector (including the null functional and operator), and we will denote by C and c, with or without subscripts, bars, tildes or hats, generic constants independent of the meshsize, but might depend on the polynomial degree, the shape-regularity of the triangulation and the domain. Moreover, for quantities A and B, we write $A \lesssim B$, whenever there exists $C > 0$ such that $A \leq CB$.

2 The Galerkin method

In this section we derive our numerical scheme and analyze its well-posedness. We begin by introducing some notations and auxiliary results.

2.1 Notation and preliminaries

For the sake of completeness and easy presentation of the main ideas, we start by briefly recalling the mixed formulation of the Poisson problem, which reads: Find $(\boldsymbol{\sigma}, u) \in \mathbf{H}(\mathrm{div}\,;\Omega) \times \mathrm{L}^2(\Omega)$ such that

$$\begin{aligned} a(\boldsymbol{\sigma},\boldsymbol{\tau}) + b(\boldsymbol{\tau}, u) &= G(\boldsymbol{\tau}) \quad \forall\, \boldsymbol{\tau} \in \mathbf{H}(\mathrm{div}\,;\Omega), \\ b(\boldsymbol{\sigma}, v) &= F(v) \quad \forall\, v \in \mathrm{L}^2(\Omega), \end{aligned} \tag{2.1}$$

where the bilinear forms $a : \mathbf{H}(\mathrm{div}\,;\Omega) \times \mathbf{H}(\mathrm{div}\,;\Omega) \to \mathbb{R}$, $b : \mathbf{H}(\mathrm{div}\,;\Omega) \times \mathrm{L}^2(\Omega) \to \mathbb{R}$, and the linear functionals $G : \mathbf{H}(\mathrm{div}\,;\Omega) \to \mathbb{R}$, $F : \mathrm{L}^2(\Omega) \to \mathbb{R}$ are defined by

$$a(\boldsymbol{\sigma},\boldsymbol{\tau}) := \int_\Omega \boldsymbol{\sigma}\cdot\boldsymbol{\tau}\, d\mathbf{x}, \quad b(\boldsymbol{\tau}, v) := \int_\Omega v \,\mathrm{div}\,\boldsymbol{\tau}\, d\mathbf{x}, \quad G(\boldsymbol{\tau}) := \langle \boldsymbol{\tau}\cdot\boldsymbol{\nu}_\Gamma, g\rangle_\Gamma, \quad F(v) := -\int_\Omega f\, v\, d\mathbf{x}.$$

Here $\boldsymbol{\nu}_\Gamma$ stands for the outward unit normal to Γ. For the well-posedness analysis of this problem we refer the reader to [21, Chapter 2].

Next, to derive our numerical method, from now on we suppose that Ω can be approximated by a family of polygonal subdomains D_h. To construct such a family, the most natural choice, guided by [15, Section 2.1], consists of considering a *background* domain $\mathcal{B} \supset \Omega$ easy to triangulate. More precisely, given a mesh $\mathcal{T}_h$ of $\overline{\mathcal{B}}$ made up of triangles K of diameter h_K, we use a level set function φ to determine which elements are inside of Ω in order to set our subdomain D_h; see an illustration in Figure 1. Here $\varphi : \mathcal{B} \to \mathbb{R}$ is a continuous function such that $\varphi < 0$ in Ω, $\varphi = 0$ in Γ and $\varphi > 0$ in $\mathcal{B} \setminus \overline{\Omega}$. Then, we define $\mathrm{T}_h := \{K \in \mathcal{T}_h :\ \varphi(\mathbf{x}) \le 0\ \forall\, \mathbf{x} \in K\}$ and set $\mathrm{D}_h := (\cup_{K\in\mathrm{T}_h}\overline{K})^\circ$. Also, we set $\Gamma_h := \partial\mathrm{D}_h$ and $\mathrm{D}_h^c := \Omega \setminus \overline{\mathrm{D}_h}$.

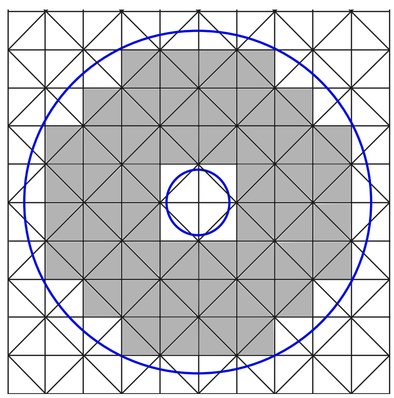

Figure 1: Example of a curved domain Ω (annulus of boundary Γ in blue color), a corresponding background domain $\mathcal{B}$, and the polygonal subdomain D_h (gray color).

Now, we introduce notation associated with the sets introduced above. Hereafter, h denotes the meshsize of the triangulation T_h of $\overline{\mathrm{D}}_h$, that is $h := \max\{h_K :\ K \in \mathrm{T}_h\}$. In addition, we denote by $\mathcal{E}_h$ the set of all edges/faces of T_h, subdivided as follows

$$\mathcal{E}_h = \mathcal{E}_h^0 \cup \mathcal{E}_h^\partial,$$

where $\mathcal{E}_h^0 := \{e \in \mathcal{E}_h :\ e \subseteq \mathrm{D}_h\}$ and $\mathcal{E}_h^\partial := \{e \in \mathcal{E}_h :\ e \subseteq \Gamma_h\}$. Finally, for all K, $\boldsymbol{\nu}_K$ will denote the the unit outward normal vector on the boundary ∂K. However, to emphasize that $\boldsymbol{\nu}$ is normal to Γ_h or to an edge e of K, we will write $\boldsymbol{\nu}_{\Gamma_h}$ or $\boldsymbol{\nu}_e$, respectively.

In the computational domain D_h, the solution of (2.1) satisfies in a distributional sense,

$$\boldsymbol{\sigma} = \nabla u \quad \text{in} \quad \mathrm{D}_h, \quad \mathrm{div}\,\boldsymbol{\sigma} = -f \quad \text{in} \quad \mathrm{D}_h. \tag{2.2}$$

Moreover, thanks to the first equation in (2.2), the trace of u on Γ_h, denoted by $\widetilde{g}$, can be written as

$$\widetilde{g}(\mathbf{x}) := \overline{g}(\mathbf{x}) - \int_{\mathscr{C}(\mathbf{x})} \boldsymbol{\sigma} \cdot \mathbf{m}(\mathbf{x})\, dr, \tag{2.3}$$

where $\mathscr{C}(\mathbf{x})$ is, in principle, any path starting at $\mathbf{x} \in \Gamma_h$ and ending at $\widetilde{\mathbf{x}} \in \Gamma$, $\mathbf{m}(\mathbf{x})$ is the unit tangent vector of $\mathscr{C}(\mathbf{x})$, and $\overline{g}(\mathbf{x}) := g(\widetilde{\mathbf{x}}(\mathbf{x}))$. In Section 2.2 we specify a construction of a suitable family of paths. Note that the value of $\widetilde{g}$ is independent of the integration path since it comes from integrating $\boldsymbol{\sigma} = \nabla u$. In addition, it is easy to see that the solution of (2.1) also satisfies

$$\begin{aligned} a_h(\boldsymbol{\sigma}, \boldsymbol{\tau}) + b_h(\boldsymbol{\tau}, u) - \langle \boldsymbol{\tau} \cdot \boldsymbol{\nu}_{\Gamma_h}, \widetilde{g} \rangle_{\Gamma_h} &= 0 \qquad && \forall\, \boldsymbol{\tau} \in \mathbf{H}(\mathrm{div}\,; \mathrm{D}_h), \\ b_h(\boldsymbol{\sigma}, v) &= F_h(v) \qquad && \forall\, v \in \mathrm{L}^2(\mathrm{D}_h), \end{aligned} \tag{2.4}$$

where the bilinear forms $a_h : \mathbf{H}(\mathrm{div}\,; \mathrm{D}_h) \times \mathbf{H}(\mathrm{div}\,; \mathrm{D}_h) \to \mathbb{R}$ and $b_h : \mathbf{H}(\mathrm{div}\,; \mathrm{D}_h) \times \mathrm{L}^2(\mathrm{D}_h) \to \mathbb{R}$, and the functional $F_h : \mathbf{H}(\mathrm{div}\,; \mathrm{D}_h) \to \mathbb{R}$ are given by

$$a_h(\boldsymbol{\sigma}, \boldsymbol{\tau}) := \int_{\mathrm{D}_h} \boldsymbol{\sigma} \cdot \boldsymbol{\tau}\, d\mathbf{x}, \quad b_h(\boldsymbol{\tau}, v) := \int_{\mathrm{D}_h} v\, \mathrm{div}\, \boldsymbol{\tau}\, d\mathbf{x}, \quad F_h(v) := -\int_{\mathrm{D}_h} f\, v\, d\mathbf{x}. \tag{2.5}$$

We end this section by mentioning that, while the classical mixed finite element method provides a Galerkin scheme for (2.1), we aim to propose a Galerkin scheme for (2.4), under a suitable approximation of the Dirichlet data on the boundary Γ_h, denoted by $\widetilde{g}_h$, allowing a high order approximation and keeping high order accuracy when the distance between Γ and Γ_h is of only order h. Before doing that, we proceed analogously to [17] and construct the aforementioned family of transferring paths.

2.2 Family of transferring paths

We now summarize the procedure introduced in [15] to construct the family of transferring paths $\{\mathscr{C}(\mathbf{x})\}_{\mathbf{x} \in \Gamma_h}$ connecting Γ_h and Γ. Let $\mathbf{u}$ and $\mathbf{v}$ be the vertices of a boundary edge e, $\mathbf{x}$ be a point on e and K^e the only element of T_h where e belongs. We first determine points $\widetilde{\mathbf{u}}$ and $\widetilde{\mathbf{v}}$ in Γ associated to $\mathbf{u}$ and $\mathbf{v}$, respectively:

***Step 1*:** For the vertex $\mathbf{u}$, we suggest two approaches to define $\widetilde{\mathbf{u}}$.

- One possibility is to use the algorithm proposed in [15, Section 2.4.1] that uniquely determines a point $\widetilde{\mathbf{u}}$ as the closest point to $\mathbf{u}$ such that $\mathscr{C}(\mathbf{u})$ does not intersect any other path and does not intersect the interior of the domain D_h. In Figure 2 (left) we display an illustration where $\widetilde{\mathbf{u}}$ is the point in Γ associated to $\mathbf{u}$.
- An alternative is to assume that Γ is $\mathcal{C}^2$ and the mesh is fine enough. In this case $\widetilde{\mathbf{u}}$ can be set as the orthogonal projections of $\mathbf{u}$ into Γ.

Let $\widehat{\mathbf{m}}^{\mathbf{u}} := \widetilde{\mathbf{u}} - \mathbf{u}$. We set $\mathbf{m}^{\mathbf{u}} := \widehat{\mathbf{m}}^{\mathbf{u}}/|\widehat{\mathbf{m}}^{\mathbf{u}}|$ if $|\widehat{\mathbf{m}}^{\mathbf{u}}| \neq 0$ and $\mathbf{m}^{\mathbf{u}} = \boldsymbol{\nu}_e$, otherwise. To define $\widetilde{\mathbf{v}}$ and $\mathbf{m}^{\mathbf{v}}$ we proceed similarly.

Then, for a point $\widetilde{\mathbf{x}} \in e$, which is not a vertex,

***Step 2*:** $\mathscr{C}(\mathbf{x})$ is determined as a convex combination of those paths originated from the vertices of e. More precisely, for $\theta \in [0,1]$, we write $\mathbf{x} = \mathbf{u}(1-\theta) + \theta\mathbf{v}$ and define $\widehat{\mathbf{m}} := \mathbf{m}^{\mathbf{u}}(1-\theta) + \theta\mathbf{m}^{\mathbf{v}}$. Then, we write $\mathbf{m} := \widehat{\mathbf{m}}/|\widehat{\mathbf{m}}|$ if $|\widehat{\mathbf{m}}| \neq 0$ and $\mathbf{m} := \boldsymbol{\nu}_e$, otherwise. Thus, we set $\widetilde{\mathbf{x}}$ as the intersection between the boundary Γ and the ray starting at $\mathbf{x}$ whose unit tangent vector is $\mathbf{m}$; see Figure 2 (right) for an illustration.

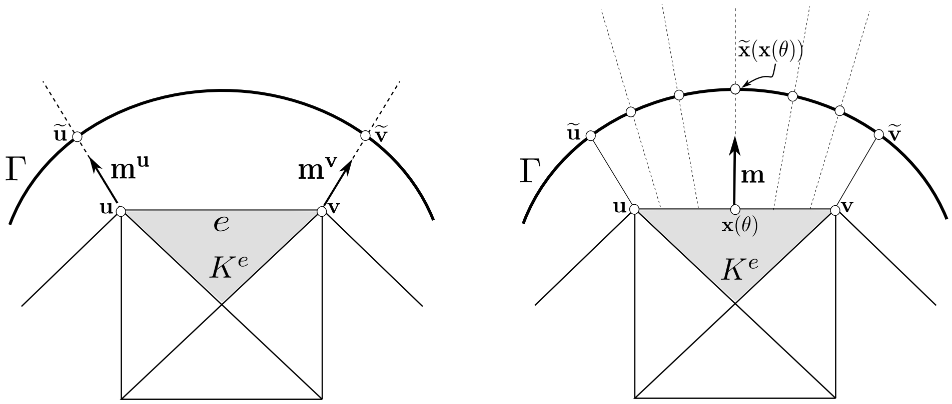

Figure 2: *Transferring paths* from the boundary edge e.

Subsequently, the transferring path connecting a point $\mathbf{x} \in \Gamma_h$ to the point $\widetilde{\mathbf{x}} := \mathbf{x} + \ell(\mathbf{x})\mathbf{m} \in \Gamma$, where $\ell(\mathbf{x}) := |\widetilde{\mathbf{x}} - \mathbf{x}|$, is given by

$$\mathscr{C}(\mathbf{x}) := \{\mathbf{x} + t\mathbf{m} : \ t \in [0, \ell(\mathbf{x})]\} . \tag{2.6}$$

Additionally, for each edge $e \in \mathcal{E}_h^\partial$ of vertices $\mathbf{u}$ and $\mathbf{v}$, we define $\widetilde{K}^e_{ext}$ as the region enclosed by the intersection of D_h^c with the cones (see Figure 3):

$$C_1 := \left\{ \mathbf{u} + \eta_1(\tilde{\mathbf{u}} - \mathbf{u}) + \eta_2(\mathbf{v} - \mathbf{u}) : \ \eta_1, \, \eta_2 \in \mathbb{R}^+ \right\},$$
$$C_2 := \left\{ \mathbf{v} + \eta_1(\tilde{\mathbf{v}} - \mathbf{v}) + \eta_2(\mathbf{u} - \mathbf{v}) : \ \eta_1, \, \eta_2 \in \mathbb{R}^+ \right\},$$

and denote by $\widetilde{\mathrm{T}}_h := \left\{ \widetilde{K}^e_{ext} : \ e \in \mathcal{E}_h^\partial \right\}$ the partition of D_h^c, satisfying,

$$\overline{\mathrm{D}_h^c} \; = \bigcup_{e \in \mathcal{E}_h^\partial} \widetilde{K}^e_{ext}.$$

2.3 Statement of the Galerkin scheme

Let us introduce generic finite dimensional subspaces $\mathbf{H}_h(\mathrm{D}_h)$ and $\mathrm{Q}_h(\mathrm{D}_h)$ of $\mathbf{H}(\mathrm{div}\,;\mathrm{D}_h)$ and $\mathrm{L}^2(\mathrm{D}_h)$, respectively. On each $K \in \mathrm{T}_h$, we let $(\mathbf{M}(K), \mathrm{W}(K))$ be a pair of arbitrary finite dimensional subspaces, where $\mathbf{M}(K)$ is the space of two-dimensional vector functions on K, and $\mathrm{W}(K)$ is the space of scalar functions on K. Then, our approach consists of approximating the exact solution $(\boldsymbol{\sigma}, u)$ by a pair $(\boldsymbol{\sigma}_h, u_h)$ belonging to the product space $\mathbf{H}_h(\mathrm{D}_h) \times \mathrm{Q}_h(\mathrm{D}_h)$, where

$$\begin{aligned} \mathbf{H}_h(\mathrm{D}_h) &:= \left\{ \boldsymbol{\tau}_h \in \mathbf{H}(\mathrm{div}\,;\mathrm{D}_h) : \ \boldsymbol{\tau}_h|_K \in \mathbf{M}(K) \quad \forall\, K \in \mathrm{T}_h \right\}, \\ \mathrm{Q}_h(\mathrm{D}_h) &:= \left\{ v_h \in \mathrm{L}^2(\mathrm{D}_h) : \ v_h|_K \in \mathrm{W}(K) \quad \forall\, K \in \mathrm{T}_h \right\}. \end{aligned} \tag{2.7}$$

A feasible choice of $(\mathbf{M}(K), \mathrm{W}(K))$ will be specified in Section 4. Now, inspired by (2.3), for any $\mathbf{x}$ lying in $e \in \mathcal{E}_h^\partial$, $\widetilde{g}$ can be approximated by

$$\widetilde{g}_h(\mathbf{x}) := \overline{g}(\mathbf{x}) - \int_0^{\ell(\mathbf{x})} \mathbf{E}_h(\boldsymbol{\sigma}_h)(\mathbf{x} + t\mathbf{m}) \cdot \mathbf{m} \, dt, \tag{2.8}$$

where $\mathbf{E}_h(\boldsymbol{\sigma}_h)$ is a local extension operator from K^e to $\widetilde{K}^e_{ext}$ acting on $\boldsymbol{\sigma}_h$. In practice, since $\mathbf{M}(K)$ is a space of polynomials, given $\boldsymbol{\zeta}_h \in \mathbf{M}(K)$ we consider $\mathbf{E}_h(\boldsymbol{\zeta}_h)$ as the extrapolation of $\boldsymbol{\zeta}_h$ from K^e to

$\widetilde{K}^e_{ext}$. In this way, defining now

$$d_h(\boldsymbol{\zeta}_h, \boldsymbol{\tau}_h) := \sum_{e\in\mathcal{E}_h^\partial} \int_e \left(\int_0^{\ell(\mathbf{x})} \mathbf{E}_h(\boldsymbol{\zeta}_h)(\mathbf{x}+t\mathbf{m}) \cdot \mathbf{m}\, dt \right) \boldsymbol{\tau}_h \cdot \boldsymbol{\nu}_e \, dS_{\mathbf{x}}, \tag{2.9}$$

and

$$G_h(\boldsymbol{\tau}_h) := \sum_{e\in\mathcal{E}_h^\partial} \int_e \overline{g}\, \boldsymbol{\tau}_h \cdot \boldsymbol{\nu}_e \, dS_{\mathbf{x}}, \tag{2.10}$$

for $\boldsymbol{\zeta}_h$, $\boldsymbol{\tau}_h \in \mathbf{H}_h(\mathrm{D}_h)$, the Galerkin scheme associated to (2.4), reads: Find $(\boldsymbol{\sigma}_h, u_h) \in \mathbf{H}_h(\mathrm{D}_h)\times \mathrm{Q}_h(\mathrm{D}_h)$ such that

$$\begin{aligned} (a_h + d_h)(\boldsymbol{\sigma}_h, \boldsymbol{\tau}_h) + b_h(\boldsymbol{\tau}_h, u_h) &= G_h(\boldsymbol{\tau}_h) \quad \forall\, \boldsymbol{\tau}_h \in \mathbf{H}_h(\mathrm{D}_h), \\ b_h(\boldsymbol{\sigma}_h, v_h) &= F_h(v_h) \quad \forall\, v_h \in \mathrm{Q}_h(\mathrm{D}_h), \end{aligned} \tag{2.11}$$

where the bilinear forms a_h, b_h and the functional F_h have been introduced in Section 2.1. We remark that problem (2.11) can be seen as the discrete version of problem (2.4) where $\widetilde{g}$ has been approximated by $\widetilde{g}_h$ (cf. (2.8)). Moreover, if Ω were a polygonal domain coinciding with D_h, the term $d_h(\boldsymbol{\zeta}_h, \boldsymbol{\tau}_h)$ would be zero for all $\boldsymbol{\zeta}_h, \boldsymbol{\tau}_h \in \mathbf{H}_h(\mathrm{D}_h)$, and then problem (2.11) would become well-posed provided the Babuška–Brezzi conditions are proved, namely, the coercivity of a_h on the kernel of b_h, the discrete inf-sup condition for b_h and the boudedness of all the forms involved.

2.4 Solvability analysis

We now aim to prove the well-posedness of problem (2.11). We begin by stating the assumptions regarding the Galerkin method, the triangulation and the *closeness* between Γ_h and Γ. Let us first introduce some assumptions on the boundary Γ and the mesh T_h.

A. For some technical results concerning inverse inequalities, we first assume that the elements K in T_h are shape-regular in the sense of Ciarlet (see [10]):

(A.1) There is a constant γ_K such that $h_K \leq \gamma_K \rho_K$, where ρ_K is the radius of the largest ball contained in K.

Next, in order to give sense to the integrals involved in G_h and d_h in (2.11), we need $\widetilde{g}_h$ (cf. (2.8)) to be a measurable function, which certainly holds under the following assumptions on the boundary Γ (see [17, Lemma 3.1]):

(A.2) Γ is a compact Lipschitz boundary,

(A.3) There exits $\widetilde{\Gamma} \subset \Gamma$ closed in Γ such that $|\widetilde{\Gamma}| = 0$ and $\Gamma\backslash\widetilde{\Gamma}$ is $\mathcal{C}^2$.

Owing to the latter hypothesis we can also define extension operators from Ω to $\mathbb{R}^2$. In fact, relaxing the smoothness requirement in assumption (A.3) to $\mathcal{C}^1$ only, we have the following extension theorem. For its proof we refer to [32, Chapter VI].

Theorem 2.1. *There is an extension mapping $\mathscr{E} : \mathrm{H}^m(\Omega) \to \mathrm{H}^m(\mathbb{R}^2)$ defined for all non-negative integers m satisfying $\mathscr{E}(\zeta)\big|_\Omega = \zeta$ for all $\zeta \in \mathrm{H}^m(\Omega)$ and*

$$\|\mathscr{E}(\zeta)\|_{m,\mathbb{R}^2} \leq C\|\zeta\|_{m,\Omega},$$

where C is independent of ζ.

In order to simplify the technicalities of the analysis on the region D_h^c, for every edge $e \in \mathcal{E}_h^\partial$ and $\mathbf{x} \in e$, we assume that

(A.4) the intersection of the ray $\{\mathbf{x} + \eta(\widetilde{\mathbf{x}} - \mathbf{x}),\ \eta \in \mathbb{R}^+\}$ with Γ is unique.

This prevents situations like the one shown at the right of Figure 3.

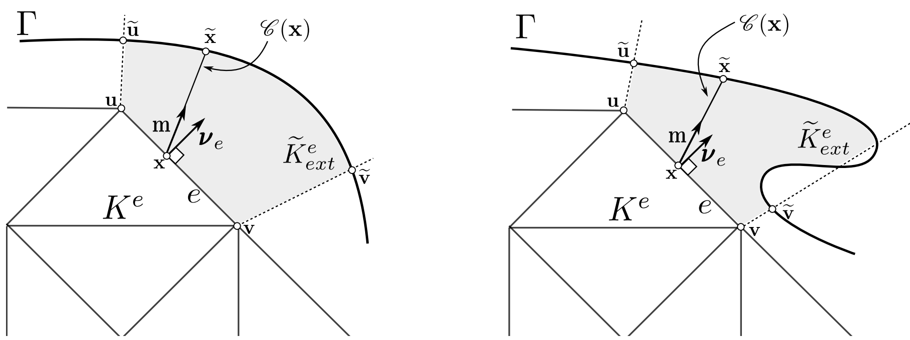

Figure 3: Examples of sets $\widetilde{K}^e_{ext}$.

Next, we describe two sets of hypothesis establishing the constraints on the choice of the discrete subspaces in (2.7).

B. Let $\mathbf{V}^{\mathrm{D}_h}$ be the discrete kernel of b_h, i.e.,

$$\mathbf{V}^{\mathrm{D}_h} = \{\boldsymbol{\tau}_h \in \mathbf{H}_h(\mathrm{D}_h) :\ b_h(\boldsymbol{\tau}_h, v_h) = 0 \quad \forall\, v_h \in \mathrm{Q}_h(\mathrm{D}_h)\}\,.$$

In order to have a more explicit definition of $\mathbf{V}^{\mathrm{D}_h}$ we introduce the following assumption:

(B.1) $\operatorname{div} \mathbf{H}_h(\mathrm{D}_h) \subseteq \mathrm{Q}_h(\mathrm{D}_h)$.

If fact, owing to (B.1) the subspace $\mathbf{V}^{\mathrm{D}_h}$ can be characterized as follows

$$\mathbf{V}^{\mathrm{D}_h} = \{\boldsymbol{\tau}_h \in \mathbf{H}_h(\mathrm{D}_h) :\ \operatorname{div} \boldsymbol{\tau}_h \equiv 0 \quad \text{in} \quad \mathrm{D}_h\}\,.$$

Consequently, the bilinear form a_h satisfies the identity

$$a_h(\boldsymbol{\tau}_h, \boldsymbol{\tau}_h) \;=\; \|\boldsymbol{\tau}_h\|^2_{\operatorname{div};\mathrm{D}_h} \quad \forall\, \boldsymbol{\tau}_h \in \mathbf{V}^{\mathrm{D}_h},$$

which clearly shows that a_h is coercive on $\mathbf{V}^{\mathrm{D}_h}$ with constant $\hat{\alpha} = 1$. In turn, we assume that b_h satisfies the inf-sup condition:

(B.2) There exists $\hat{\beta} > 0$, independent of h, such that

$$\sup_{\substack{\boldsymbol{\tau}_h \in \mathbf{H}_h(\mathrm{D}_h) \\ \boldsymbol{\tau}_h \neq \mathbf{0}}} \frac{b_h(\boldsymbol{\tau}_h, v_h)}{\|\boldsymbol{\tau}_h\|_{\operatorname{div};\mathrm{D}_h}} \;\geq\; \hat{\beta} \|v_h\|_{0,\mathrm{D}_h} \quad \forall\, v_h \in \mathrm{Q}_h(\mathrm{D}_h).$$

For the subsequent analysis we will also need the following hypotheses on the local discrete spaces.

C. Given an integer $k \geq 0$ and a region $\mathcal{O} \subset \mathbb{R}^2$, we denote by $\mathrm{P}_k(\mathcal{O})$ the space of polynomials of degree at most k defined on $\mathcal{O}$, and let $\mathbf{P}_k(\mathcal{O}) := [\mathrm{P}_k(\mathcal{O})]^2$. Let n_1, n_2 and n_3 be integers such that n_1, $n_2 \geq 1$ and $n_3 \geq 0$. Then, for all $e \in \mathcal{E}_h^\partial$, (C.1) $\mathbf{M}(K^e) \subseteq \mathbf{P}_{n_1}(K^e)$,

(C.2) $\mathbf{M}(K^e)\cdot \boldsymbol{\nu}_{K^e}|_{\widetilde{e}} \subseteq \mathrm{P}_{n_2}(\widetilde{e})$ for all edge $\widetilde{e} \subset \partial K^e$,

(C.3) $\mathrm{W}(K^e) \subseteq \mathrm{P}_{n_3}(K^e)$,

Next, in Section 4 we specify suitable choices of finite element subspaces satisfying hypotheses (B.1), (B.2) and (C.1)–(C.3).

Now we introduce assumptions related to the sets $\widetilde{K}^e_{ext}$ and the bilinear form d_h. More precisely, in what follows we introduce smallness assumptions on certain quantities that will appear in the analysis of our method when approximating the L^2-norm of functions defined on $\widetilde{K}^e_{ext}$. These conditions determine how close the boundaries Γ and Γ_h must be.

D. Let e be any edge in $\mathcal{E}_h^\partial$. We define $\widetilde{r}_e := \widetilde{H}_e/h_e^\perp$, where $\widetilde{H}_e := \max_{\boldsymbol{x}\in e} \ell(\boldsymbol{x})$ and $h_e^\perp$ is the distance between the vertex of K^e, opposite to e, and the plane determined by e. We assume

(D.1) $\widetilde{r}_e \leq R$,

where R denotes a constant that does not depend on the meshsize h. This hypothesis indicates that the distance $d(\Gamma,\Gamma_h)$ must be at most $\mathcal{O}(h)$. In particular, the family of paths (Σ_h) (cf. Section 2.2) satisfies this hypothesis by construction.

To establish the remaining hypotheses, for each $K \in \mathrm{T}_h$ we denote

$$\mathrm{N}_h(\partial K) = \Big\{ w \in \mathrm{L}^2(\partial K) : w|_e \in \mathrm{P}_{n_2}(e) \text{ for all edges } e \text{ of } K \Big\},$$

and introduce the following constant:

$$C^e_{eq} := h_{K^e}^{1/2} \sup_{\substack{w_h \in \mathrm{N}_h(\partial K^e)\\ w_h \neq 0}} \frac{\|w_h\|_{0,\partial K^e}}{\|w_h\|_{-1/2,\partial K^e}}. \tag{2.12}$$

This definition can be inferred using the *equivalence* of the norms $\|\cdot\|_{0,\partial K}$ and $\|\cdot\|_{-1/2,\partial K}$ on the space $\mathrm{N}_h(\partial K)$ for all $K \in \mathrm{T}_h$; see [18, Lemma 3.2] for further details. Moreover, the value of C^e_{eq} depends solely on the shape-regularity constant γ_{K^e} and the polynomial degree of the space $\mathrm{N}_h(\partial K^e)$.

We shall also make frequent use of the quantity

$$|||\mathbf{p}|||_e := \left(\int_e \int_0^{\ell(\mathbf{x})} |\mathbf{p}(\mathbf{x} + t\mathbf{m}(\mathbf{x}))|^2 \, dt \, dS_{\mathbf{x}} \right)^{1/2}, \tag{2.13}$$

where $e \in \mathcal{E}_h^\partial$ and $\mathbf{p}$ is smooth enough in order to make the integral well-defined. In addition, we define

$$\widetilde{C}^e_{ext} := \widetilde{r}_e^{-1/2} \sup_{\substack{\boldsymbol{\zeta}_h \in \mathbf{M}(K^e)\\ \boldsymbol{\zeta}_h \neq \mathbf{0}}} \frac{|||\mathbf{E}_h(\boldsymbol{\zeta}_h)|||_e}{\|\boldsymbol{\zeta}_h\|_{0,K^e}}. \tag{2.14}$$

We recall that $\mathbf{E}_h(\boldsymbol{\zeta}_h)$ is the extrapolation of the polynomial $\boldsymbol{\zeta}_h$ from K^e to $\widetilde{K}^e_{ext}$, since if $\mathbf{M}(K^e)$ is a space of polynomials thanks to (C.1). The constant $\widetilde{C}^e_{ext}$ is independent of the meshsize h, but depends on the shape-regularity constant γ_{K^e} and on the polynomial degree; see Appendix A.

We are now in a position of discussing the boundedness of the bilinear form d_h. Let $\boldsymbol{\zeta}_h \in \mathbf{H}_h(\mathrm{D}_h)$. According to the notations stated in Section 2.2, for any $\mathbf{x}$ lying on a boundary edge e, we set

$$\widetilde{w}_h(\mathbf{x}) := \int_0^{\ell(\mathbf{x})} \mathbf{E}_h(\boldsymbol{\zeta}_h)(\mathbf{x} + t\,\mathbf{m}(\mathbf{x}))\cdot \mathbf{m}(\mathbf{x})\, dt.$$

Applying the Cauchy–Schwarz inequality, considering (2.13), (2.14) and the fact that, for all $\mathbf{x} \in e$, $\ell(\mathbf{x}) \le \widetilde{H}_e = \widetilde{r}_e h_e^{\perp} \le \widetilde{r}_e h_{K^e}$, we obtain

$$\begin{aligned}\|\widetilde{w}_h\|_{0,e}^2 &\le \int_e \ell(\mathbf{x}) \int_0^{\ell(\mathbf{x})} |\mathbf{E}_h(\boldsymbol{\zeta}_h)|^2(\mathbf{x} + t\mathbf{m}(\mathbf{x}))\, dt\, dS_{\mathbf{x}} \\ &\le \widetilde{r}_e \widetilde{H}_e \left(\widetilde{C}_{ext}^e\right)^2 \|\boldsymbol{\zeta}_h\|_{0,K^e}^2 \\ &\le \widetilde{r}_e^2 h_{K_e} \left(\widetilde{C}_{ext}^e\right)^2 \|\boldsymbol{\zeta}_h\|_{0,K^e}^2 .\end{aligned} \tag{2.15}$$

In turn, by definition of d_h (cf. (2.9)), utilizing again the Cauchy–Schwarz inequality, and using definition (2.12) together with assumption (C.2), we deduce that

$$|d_h(\boldsymbol{\zeta}_h, \boldsymbol{\tau}_h)| \le \sum_{e\in\mathcal{E}_h^\partial} \|\widetilde{w}_h\|_{0,e} \|\boldsymbol{\tau}_h \cdot \boldsymbol{\nu}_e\|_{0,\partial K^e} \le \max_{e\in\mathcal{E}_h^\partial} \left\{\widetilde{r}_e \widetilde{C}_{ext}^e C_{eq}^e\right\} \|\boldsymbol{\zeta}_h\|_{\mathrm{div}\,;\mathrm{D}_h} \|\boldsymbol{\tau}_h\|_{\mathrm{div}\,;\mathrm{D}_h}, \tag{2.16}$$

for all $\boldsymbol{\zeta}_h, \boldsymbol{\tau}_h \in \mathbf{H}_h(\mathrm{D}_h)$, where we have utilized the continuity of the normal trace operator acting from $\mathbf{H}(\mathrm{div}\,; K^e)$ onto $\mathrm{H}^{-1/2}(\partial K^e)$ (see e.g. [21, Theorem 1.7]). Thus, the boundedness of d_h is certainly satisfied if we assume that:

(D.2)

$$\max_{e\in\mathcal{E}_h^\partial} \left\{\widetilde{r}_e \widetilde{C}_{ext}^e C_{eq}^e\right\} \le 1/2.$$

We emphasize that, in general, the condition above is not entirely verifiable because, in most cases, some of the quantities involved cannot be calculable explicitly. Certainly it holds if $\widetilde{r}_e$ for h is small enough, as it happens when the boundary is interpolated by a piecewise linear function.

Having introduced the aforementioned hypotheses we are now in position of establishing the main result of this section, namely, the well-posedness of problem (2.11).

Theorem 2.2. *Suppose that assumptions* **A**, **B**, **C** *and* **D** *are satisfied. Then, given $f \in \mathrm{L}^2(\Omega)$ and $g \in \mathrm{H}^{1/2}(\Gamma)$, there exists a unique $(\boldsymbol{\sigma}_h, u_h) \in \mathbf{H}_h(\mathrm{D}_h) \times \mathrm{Q}_h(\mathrm{D}_h)$ solution to problem (2.11) which satisfies*

$$\|(\boldsymbol{\sigma}_h, u_h)\|_{\mathbf{H}(\mathrm{div}\,;\mathrm{D}_h)\times \mathrm{L}^2(\mathrm{D}_h)} \le C \left\{ \sup_{\substack{w_h \in \mathrm{Q}_h(\mathrm{D}_h)\\ w_h \neq 0}} \frac{|F_h(w_h)|}{\|w_h\|_{0,\mathrm{D}_h}} + \sup_{\substack{\boldsymbol{\zeta}_h \in \mathbf{H}_h(\mathrm{D}_h)\\ \boldsymbol{\zeta}_h \neq \mathbf{0}}} \frac{|G_h(\boldsymbol{\zeta}_h)|}{\|\boldsymbol{\zeta}_h\|_{\mathrm{div}\,;\mathrm{D}_h}} \right\}.$$

Proof. Let us start by providing the boundedness of the forms involved. Since $\widetilde{\mathbf{x}} : \Gamma_h \to \Gamma$ is a continuous mapping and we have assumed $g \in \mathrm{H}^{1/2}(\Gamma)$, the composition $\overline{g}(\cdot) := g(\widetilde{\mathbf{x}}(\cdot))$ is a function in $\mathrm{H}^{1/2}(\Gamma_h)$, and then we can apply the normal trace theorem (see e.g. [21, Theorem 1.7]) to obtain $|G_h(\boldsymbol{\tau}_h)| \le \|\boldsymbol{\tau}_h\|_{\mathrm{div}\,;\mathrm{D}_h} \|\overline{g}\|_{1/2,\Gamma_h}$ for all $\boldsymbol{\tau}_h \in \mathbf{H}_h(\mathrm{D}_h)$, which implies G_h bounded with constant $\|G_h\| \le 1$. Moreover, we easily obtain a_h, b_h and F_h bounded with constants ≤ 1.

On the other hand, the bilinear form $a_h + d_h$ is coercive on $\mathbf{V}^{\mathrm{D}_h}$. Indeed, it is clear that

$$(a_h + d_h)(\boldsymbol{\tau}_h, \boldsymbol{\tau}_h) \ge \frac{1}{2} \|\boldsymbol{\tau}_h\|_{\mathrm{div}\,;\mathrm{D}_h}^2 \quad \forall\, \boldsymbol{\tau}_h \in \mathbf{V}^{\mathrm{D}_h},$$

owing to (2.16), assumptions (B.1) and (D.2), confirming the assertion. Finally, the discrete inf-sup condition for b_h is fulfilled by virtue of assumption (B.2) and hence the result is a straightforward consequence of the classical Babuška–Brezzi theory. ∎

3 Error analysis

In this section we carry out the error analysis for our Galerkin scheme (2.11). We first derive error estimates on D_h by considering the arbitrary finite element subspaces satisfying the assumptions in Section 2.4, and well-known Strang-type estimates for saddle point problems. Then, we will follow the procedure in [17, Section 5.2] to control the errors on D_h^c. Moreover, we use the aforementioned analysis to state the theoretical rates of convergence when using the specific discrete spaces provided in Section 4.

3.1 Error estimates on D_h

Let $(\boldsymbol{\sigma}, u) \in \mathbf{H}(\mathrm{div}\,;\Omega) \times \mathrm{L}^2(\Omega)$ be the solution of (2.1) satisfying (2.4) and let $(\boldsymbol{\sigma}_h, u_h) \in \mathbf{H}_h(\mathrm{D}_h) \times \mathrm{Q}_h(\mathrm{D}_h)$ be the solution of (2.11). Firstly, we are interested in obtaining upper bounds for

$$\|(\boldsymbol{\sigma}, u) - (\boldsymbol{\sigma}_h, u_h)\|_{\mathbf{H}(\mathrm{div}\,;\mathrm{D}_h)\times \mathrm{L}^2(\mathrm{D}_h)}.$$

To this end, we rearrange (2.4) and (2.11) as the following pairs of continuous and discrete formulations:

$$\begin{aligned} a_h(\boldsymbol{\sigma}, \boldsymbol{\tau}) + b_h(\boldsymbol{\tau}, u) &= \langle \boldsymbol{\tau}\cdot\boldsymbol{\nu}_{\Gamma_h}, \widetilde{g}\rangle_{\Gamma_h} && \forall\, \boldsymbol{\tau} \in \mathbf{H}(\mathrm{div}\,;\mathrm{D}_h),\\ b_h(\boldsymbol{\sigma}, v) &= F_h(v) && \forall\, v \in \mathrm{L}^2(\mathrm{D}_h), \end{aligned} \tag{3.1}$$

and

$$\begin{aligned} a_h(\boldsymbol{\sigma}_h, \boldsymbol{\tau}_h) + b_h(\boldsymbol{\tau}_h, u_h) &= G_h(\boldsymbol{\tau}_h) - d_h(\boldsymbol{\sigma}_h, \boldsymbol{\tau}_h) && \forall\, \boldsymbol{\tau}_h \in \mathbf{H}_h(\mathrm{D}_h),\\ b_h(\boldsymbol{\sigma}_h, v_h) &= F_h(v_h) && \forall\, v_h \in \mathrm{Q}_h(\mathrm{D}_h). \end{aligned} \tag{3.2}$$

Thus, as we have already pointed out before and as suggested by the structure of the foregoing systems, in what follows we proceed similarly to [22] (see also [11]) and apply a Strang-type estimate for saddle point problems whose continuous and discrete schemes differ only in the functionals involved, which for the sake of completeness is introduced next. We refer the reader to [30, Theorem 11.2] for more details.

Theorem 3.1. *Let $\mathbf{H}$ and Q be two Hilbert spaces, $\mathcal{G} \in \mathbf{H}'$, $\mathcal{F} \in \mathrm{Q}'$, and let $a : \mathbf{H}\times\mathbf{H} \to \mathbb{R}$ and $b : \mathbf{H}\times\mathrm{Q} \to \mathbb{R}$ be bounded bilinear forms satisfying the Babuška–Brezzi conditions, that is,*

(i) There exists $\alpha > 0$ such that

$$a(\boldsymbol{\tau}, \boldsymbol{\tau}) \geq \alpha \|\boldsymbol{\tau}\|_{\mathbf{H}}^2 \quad \forall\, \boldsymbol{\tau} \in \mathbf{V},$$

where $\mathbf{V} := \{\boldsymbol{\tau} \in \mathbf{H} :\ b(\boldsymbol{\tau}, v) = 0 \quad \forall\, v \in \mathrm{Q}\}$.

(ii) There exists $\beta > 0$ such that

$$\sup_{\substack{\boldsymbol{\tau}\in\mathbf{H}\\ \boldsymbol{\tau}\neq\mathbf{0}}} \frac{b(\boldsymbol{\tau}, v)}{\|\boldsymbol{\tau}\|_{\mathbf{H}}} \geq \beta \|v\|_{\mathrm{Q}} \quad \forall\, v \in \mathrm{Q}.$$

In addition, let $\mathbf{H}_h$ and Q_h be two finite dimensional subspaces of $\mathbf{H}$ and Q, respectively, and for each $h > 0$ consider functionals $\mathcal{G}_h \in \mathbf{H}_h'$ and $\mathcal{F}_h \in \mathrm{Q}_h'$. Assume that:

(iii) There exists $\hat{\alpha} > 0$, independent of the discretization parameter h, such that

$$a(\boldsymbol{\tau}_h, \boldsymbol{\tau}_h) \geq \hat{\alpha} \|\boldsymbol{\tau}_h\|_{\mathbf{H}}^2 \quad \forall\, \boldsymbol{\tau}_h \in \mathbf{V}_h,$$

where $\mathbf{V}_h := \{\boldsymbol{\tau}_h \in \mathbf{H}_h :\ b(\boldsymbol{\tau}_h, v_h) = 0 \quad \forall\, v_h \in \mathrm{Q}_h\}$.

(iv) *There exists $\hat{\beta} > 0$, independent of the discretization parameter h, such that*

$$\sup_{\substack{\boldsymbol{\tau}_h \in \mathbf{H}_h \\ \boldsymbol{\tau}_h \neq \mathbf{0}}} \frac{b(\boldsymbol{\tau}_h, v_h)}{\|\boldsymbol{\tau}_h\|_{\mathbf{H}}} \geq \hat{\beta} \|v_h\|_{\mathrm{Q}} \quad \forall\, v_h \in \mathrm{Q}_h.$$

In turn, let $(\boldsymbol{\sigma}, u) \in \mathbf{H} \times \mathrm{Q}$ and $(\boldsymbol{\sigma}_h, u_h) \in \mathbf{H}_h \times \mathrm{Q}_h$ such that

$$\begin{aligned} a(\boldsymbol{\sigma}, \boldsymbol{\tau}) + b(\boldsymbol{\tau}, u) &= \mathcal{G}(\boldsymbol{\tau}) \quad \forall\, \tau \in \mathbf{H}, \\ b(\boldsymbol{\sigma}, v) &= \mathcal{F}(v) \quad \forall\, v \in \mathrm{Q}, \end{aligned} \tag{3.3}$$

and

$$\begin{aligned} a(\boldsymbol{\sigma}_h, \boldsymbol{\tau}_h) + b(\boldsymbol{\tau}_h, u_h) &= \mathcal{G}_h(\boldsymbol{\tau}_h) \quad \forall\, \boldsymbol{\tau}_h \in \mathbf{H}_h, \\ b(\boldsymbol{\sigma}_h, v_h) &= \mathcal{F}_h(v_h) \quad \forall\, v_h \in \mathrm{Q}_h. \end{aligned} \tag{3.4}$$

Then, for each $h > 0$ the following estimates hold

$$\begin{aligned} \|\boldsymbol{\sigma} - \boldsymbol{\sigma}_h\|_{\mathrm{div}\,;\mathrm{D}_h} \leq{} & \left(1 + \frac{\|a\|}{\hat{\alpha}}\right)\left(1 + \frac{\|b\|}{\hat{\beta}}\right) \inf_{\boldsymbol{\zeta}_h \in \mathbf{H}_h} \|\boldsymbol{\sigma} - \boldsymbol{\zeta}_h\|_{\mathbf{H}} + \frac{\|b\|}{\hat{\alpha}} \inf_{w_h \in \mathrm{Q}_h} \|u - w_h\|_{\mathrm{Q}} \\ & + \frac{1}{\hat{\beta}}\left(1 + \frac{\|a\|}{\hat{\alpha}}\right) \sup_{\substack{w_h \in \mathrm{Q}_h \\ w_h \neq 0}} \frac{|(\mathcal{F} - \mathcal{F}_h)(w_h)|}{\|w_h\|_{\mathrm{Q}}} + \left(\frac{1}{\hat{\alpha}}\right) \sup_{\substack{\boldsymbol{\tau}_h \in \mathbf{H}_h \\ \boldsymbol{\tau}_h \neq \mathbf{0}}} \frac{\big|(\mathcal{G} - \mathcal{G}_h)(\boldsymbol{\tau}_h)\big|}{\|\boldsymbol{\tau}_h\|_{\mathbf{H}}}, \end{aligned} \tag{3.5}$$

and

$$\begin{aligned} \|u - u_h\|_{0,\mathrm{D}_h} \leq{} & \frac{\|a\|}{\hat{\beta}}\left(1 + \frac{\|a\|}{\hat{\alpha}}\right)\left(1 + \frac{\|b\|}{\hat{\beta}}\right) \inf_{\boldsymbol{\zeta}_h \in \mathbf{H}_h} \|\boldsymbol{\sigma} - \boldsymbol{\zeta}_h\|_{\mathbf{H}} \\ & + \left(1 + \frac{\|b_h\|}{\hat{\beta}} + \frac{\|b\|}{\hat{\beta}}\frac{\|a\|}{\hat{\alpha}}\right) \inf_{w_h \in \mathrm{Q}_h} \|u - w_h\|_{\mathrm{Q}} \\ & + \frac{\|a\|}{\hat{\beta}^2}\left(1 + \frac{\|a\|}{\hat{\alpha}}\right) \sup_{\substack{w_h \in \mathrm{Q}_h \\ w_h \neq 0}} \frac{|(\mathcal{F} - \mathcal{F}_h)(w_h)|}{\|w_h\|_{\mathrm{Q}}} \\ & + \frac{1}{\hat{\beta}}\left(1 + \frac{\|a\|}{\hat{\alpha}}\right) \sup_{\substack{\boldsymbol{\tau}_h \in \mathbf{H}_h \\ \boldsymbol{\tau}_h \neq \mathbf{0}}} \frac{\big|(\mathcal{G} - \mathcal{G}_h)(\boldsymbol{\tau}_h)\big|}{\|\boldsymbol{\tau}_h\|_{\mathbf{H}}}. \end{aligned} \tag{3.6}$$

Hence, applying (3.5) and (3.6) to (3.1) and (3.2), noticing that in our case $\hat{\alpha} = 1$ and $\|a\| \leq 1$, we can easily deduce that

$$\|\boldsymbol{\sigma} - \boldsymbol{\sigma}_h\|_{\mathrm{div}\,;\mathrm{D}_h} \leq C_S^1 \inf_{\boldsymbol{\zeta}_h \in \mathbf{H}_h(\mathrm{D}_h)} \|\boldsymbol{\sigma} - \boldsymbol{\zeta}_h\|_{\mathrm{div}\,;\mathrm{D}_h} + C_S^2 \inf_{w_h \in \mathrm{Q}_h(\mathrm{D}_h)} \|u - w_h\|_{0,\mathrm{D}_h} + \mathbb{T}^{\boldsymbol{\sigma}}, \tag{3.7}$$

and

$$\|u - u_h\|_{0,\mathrm{D}_h} \leq C_S^3 \inf_{\boldsymbol{\zeta}_h \in \mathbf{H}_h(\mathrm{D}_h)} \|\boldsymbol{\sigma} - \boldsymbol{\zeta}_h\|_{\mathrm{div}\,;\mathrm{D}_h} + C_S^4 \inf_{w_h \in \mathrm{Q}_h(\mathrm{D}_h)} \|u - w_h\|_{0;\mathrm{D}_h} + \frac{2}{\hat{\beta}}\mathbb{T}^{\boldsymbol{\sigma}}, \tag{3.8}$$

with C_S^1, C_S^2, C_S^3 and C_S^4 being positive constants independent of the discretization parameters and

$$\mathbb{T}^{\boldsymbol{\sigma}} := \sup_{\substack{\boldsymbol{\tau}_h \in \mathbf{H}_h(\mathrm{D}_h) \\ \boldsymbol{\tau}_h \neq \mathbf{0}}} \frac{\big|\langle \boldsymbol{\tau}_h \cdot \boldsymbol{\nu}_{\Gamma_h}, \widetilde{g} \rangle_{\Gamma_h} - (G_h(\boldsymbol{\tau}_h) - d_h(\boldsymbol{\sigma}_h, \boldsymbol{\tau}_h))\big|}{\|\boldsymbol{\tau}_h\|_{\mathrm{div}\,;\mathrm{D}_h}}. \tag{3.9}$$

We now proceed to bound $\mathbb{T}^{\boldsymbol{\sigma}}$.

Lemma 3.2. *There exists a positive constant C, independent of h, such that*

$$\mathbb{T}^{\boldsymbol{\sigma}} \quad \leq \quad \inf_{\boldsymbol{\zeta}_h \in \mathbf{H}_h(\mathrm{D}_h)} \left(\sum_{e \in \mathcal{E}_h^{\partial}} (\widetilde{r}_e)^{1/2} C_{eq}^e \|\boldsymbol{\sigma} - \mathbf{E}_h(\boldsymbol{\zeta}_h)\|_e + \frac{1}{2}\|\boldsymbol{\sigma} - \boldsymbol{\zeta}_h\|_{\mathrm{D}_h} \right) + \frac{1}{2}\|\boldsymbol{\sigma} - \boldsymbol{\sigma}_h\|_{\mathrm{D}_h} \tag{3.10}$$

Proof. First of all, using the Cauchy–Schwarz inequality, (2.8) and (2.12), we immediately have that

$$\mathbb{T}^{\boldsymbol{\sigma}} \leq \sum_{e \in \mathcal{E}_h^{\partial}} C_{eq}^e h_{K^e}^{-1/2} \|\widetilde{g} - \widetilde{g}_h\|_{0,e}. \tag{3.11}$$

Moreover, for $e \in \mathcal{E}_h^{\partial}$, from the definitions of $\widetilde{g}$ and $\widetilde{g}_h$ (resp. (2.3) and (2.8)), we obtain that

$$(\widetilde{g} - \widetilde{g}_h)(\mathbf{x}) = -\int_0^{\ell(\mathbf{x})} (\boldsymbol{\sigma} - \mathbf{E}_h(\boldsymbol{\sigma}_h))(\mathbf{x} + t\mathbf{m}(\mathbf{x})) \cdot \mathbf{m}(\mathbf{x})\, dt,$$

for each point $\mathbf{x}$ of e. Then, by Cauchy–Schwarz inequality, we find that

$$\|\widetilde{g} - \widetilde{g}_h\|_{0,e}^2 \leq \widetilde{H}_e \|\boldsymbol{\sigma} - \mathbf{E}_h(\boldsymbol{\sigma}_h)\|_e^2 \leq \widetilde{r}_e h_{K^e} \|\boldsymbol{\sigma} - \mathbf{E}_h(\boldsymbol{\sigma}_h)\|_e^2,$$

which, together with (3.11), yields

$$\mathbb{T}^{\boldsymbol{\sigma}} \leq \sum_{e \in \mathcal{E}_h^{\partial}} (\widetilde{r}_e)^{1/2} C_{eq}^e \|\boldsymbol{\sigma} - \mathbf{E}_h(\boldsymbol{\sigma}_h)\|_e.$$

Let now $\boldsymbol{\zeta}_h \in \mathbf{H}_h(\mathrm{D}_h)$. Adding and subtracting $\mathbf{E}_h(\boldsymbol{\zeta}_h)$ to the term on the right hand side of last inequality, considering (2.14) and Assumption (D.2), we obtain

$$\begin{aligned}
\mathbb{T}^{\boldsymbol{\sigma}} \quad &\leq \quad \sum_{e \in \mathcal{E}_h^{\partial}} (\widetilde{r}_e)^{1/2} C_{eq}^e \|\boldsymbol{\sigma} - \mathbf{E}_h(\boldsymbol{\zeta}_h)\|_e + \sum_{e \in \mathcal{E}_h^{\partial}} (\widetilde{r}_e)^{1/2} C_{eq}^e \|\mathbf{E}_h(\boldsymbol{\zeta}_h) - \mathbf{E}_h(\boldsymbol{\sigma}_h)\|_e \\
&\leq \quad \sum_{e \in \mathcal{E}_h^{\partial}} (\widetilde{r}_e)^{1/2} C_{eq}^e \|\boldsymbol{\sigma} - \mathbf{E}_h(\boldsymbol{\zeta}_h)\|_e + \frac{1}{2} \sum_{e \in \mathcal{E}_h^{\partial}} \|\boldsymbol{\zeta}_h - \boldsymbol{\sigma}_h\|_{0,K^e}.
\end{aligned}$$

Thus, adding and subtracting $\boldsymbol{\sigma}$ we obtain (3.10). ∎

In summary, (3.7), (3.8) and (3.10), yield the following result.

Theorem 3.3. *Suppose that assumptions of Theorem 2.2 are satisfied. Let $(\boldsymbol{\sigma}, u) \in \mathbf{H}(\mathrm{div}\,;\Omega) \times \mathrm{L}^2(\Omega)$ be the solution of (2.1) satisfying (2.4) and $(\boldsymbol{\sigma}_h, u_h) \in \mathbf{H}_h(\mathrm{D}_h) \times \mathrm{Q}_h(\mathrm{D}_h)$ be the solution of (2.11). Then,*

$$\begin{aligned}
&\|(\boldsymbol{\sigma}, u) - (\boldsymbol{\sigma}_h, u_h)\|_{\mathbf{H}(\mathrm{div}\,;\mathrm{D}_h) \times \mathrm{L}^2(\mathrm{D}_h)} \\
&\qquad \lesssim \inf_{w_h \in \mathrm{Q}_h(\mathrm{D}_h)} \|u - w_h\|_{0,\mathrm{D}_h} + \inf_{\boldsymbol{\zeta}_h \in \mathbf{H}_h(\mathrm{D}_h)} \left(\|\boldsymbol{\sigma} - \boldsymbol{\zeta}_h\|_{\mathrm{div}\,;\mathrm{D}_h} + \sum_{e \in \mathcal{E}_h^{\partial}} (\widetilde{r}_e)^{1/2} C_{eq}^e \|\boldsymbol{\sigma} - \mathbf{E}_h(\boldsymbol{\zeta}_h)\|_e \right).
\end{aligned} \tag{3.12}$$

3.2 Approximating $\boldsymbol{\sigma}$ and u in D_h^c

In this section we provide error estimates outside the computational domain. Before doing so, we need to show that, under certain conditions, the norms $\|\cdot\|_{0,\widetilde{K}^e_{ext}}$ and $|||\cdot|||_e$ are equivalent.

Let $\mathbf{u}$ and $\mathbf{v}$ be the vertices of a boundary edge e, and $\tilde{\mathbf{u}}$ and $\tilde{\mathbf{v}}$ be their corresponding points in Γ described in Section 2.2. We recall that $\widetilde{K}^e_{ext}$ is the region determined by $\mathbf{u}$, $\mathbf{v}$, $\tilde{\mathbf{u}}$ and $\tilde{\mathbf{v}}$ as Figure 3 (left) shows. Then, a point $\mathbf{x}$ on e can be represented as $\mathbf{x}(\theta) = \mathbf{u} + \theta(\mathbf{v}-\mathbf{u})$ for $\theta \in [0,1]$. Now, according to Section 2.2, the tangent vector of the path associated to $\mathbf{x}$ can be written as $\widehat{\mathbf{m}}(\theta) := \mathbf{m}^{\mathbf{u}} + \theta(\mathbf{m}^{\mathbf{v}} - \mathbf{m}^{\mathbf{u}})$. Moreover, $\mathbf{m}(\theta) := \widehat{\mathbf{m}}(\theta)/|\widehat{\mathbf{m}}(\theta)|$ if $\widehat{\mathbf{m}}(\theta) \neq \mathbf{0}$; and $\mathbf{m}(\theta) = \boldsymbol{\nu}_e$, otherwise.

Thus, for $\mathbf{y} \in \widetilde{K}^e_{ext}$ we have:

$$\mathbf{y}(\theta, s) = \mathbf{x}(\theta) + \mathbf{m}(\theta)s \quad s \in [0, \ell(\theta)],\, \theta \in [0,1], \tag{3.13}$$

where $\ell(\theta)$ is the length of the transferring associated to $\mathbf{x}(\theta)$.

Now, for a vector $\mathbf{w} = (w_1, w_2)$, we define $\mathbf{w}^\perp := (-w_2, w_1)$ and the Jacobian of the above transformation is given by

$$\mathbf{J}(s,\theta) = \left| |e|\mathbf{m}(\theta)\cdot\boldsymbol{\nu}_e + \frac{s}{\alpha(\theta)}\mathbf{m}(\theta)\cdot(\mathbf{m}^{\mathbf{v}} - \mathbf{m}^{\mathbf{u}})^\perp \right|, \tag{3.14}$$

where $\alpha(\theta) = |\widehat{\mathbf{m}}(\theta)|$ if $\widehat{\mathbf{m}}(\theta) \neq \mathbf{0}$; and $\alpha(\theta) = 1$, otherwise. In turn, considering the parametrization (3.13), we have that

$$\|\mathbf{p}\|^2_{0,\widetilde{K}^e_{ext}} = \int_{\widetilde{K}^e_{ext}} |\mathbf{p}(\mathbf{y})|^2\, d\mathbf{y} = \int_0^1 \int_0^{\ell(\theta)} |\mathbf{p}(\mathbf{y}(s,\theta))|^2 |\mathbf{J}(s,\theta)|\, ds\, d\theta. \tag{3.15}$$

Thus, the equivalence of norms holds if $|\mathbf{J}(s,\theta)|$ is bounded from above and below for which specific conditions must be satisfied by the vectors appearing in (3.14). More precisely, we have,

Lemma 3.4. *Let $\mathbf{p} \in \mathrm{L}^2(\widetilde{K}^e_{ext})$ and suppose assumptions (A.1)-(A.5) are satisfied. In addition, let us consider the following conditions:*

(i) $\mathbf{m}^{\mathbf{u}} \cdot \mathbf{m}^{\mathbf{v}} \geq 0$,

(ii) there exists constant β_e, independent of h, such that $\mathbf{m}(\theta)\cdot\boldsymbol{\nu}_e \geq \beta_e > 0$ for all $\theta \in [0,1]$; and

(iii) $\mathbf{m}^{\mathbf{u}} \cdot (\mathbf{m}^{\mathbf{v}})^\perp \geq 0$.

If (i) holds, then

$$\|\mathbf{p}\|_{0,\widetilde{K}^e_{ext}} \leq C_2^e |||\mathbf{p}|||_e, \tag{3.16}$$

where $C_2^e = \left(1 + 2\sqrt{2}\,\gamma_{K^e}\widetilde{r}_e\right)^{1/2}$. Moreover, if (ii) and (iii) hold, then

$$C_1^e |||\mathbf{p}|||_e \leq \|\mathbf{p}\|_{0,\widetilde{K}^e_{ext}}, \tag{3.17}$$

with $C_1^e = \beta_e^{1/2}$.

We point out that, if $\mathbf{m}^{\mathbf{u}}$ is parallel to $\mathbf{m}^{\mathbf{v}}$, then $|\mathbf{J}(s,\theta)| = |e|$, which means that $|||\mathbf{p}|||_e = \|\mathbf{p}\|_{0,\widetilde{K}^e_{ext}}$ and conditions (i)-(iii) are not required.

Proof. By assumption (i) we have that

$$\alpha(\theta)^2 = \theta^2 + (\theta-1)^2 + 2\theta(1-\theta)\mathbf{m}^{\mathbf{u}}\cdot\mathbf{m}^{\mathbf{v}} \geq \theta^2 + (\theta-1)^2 \geq 1/2.$$

Since $\ell(\theta) \leq \widetilde{H}_e \leq \widetilde{r}_e h_{K_e} \leq \gamma_{K^e}\widetilde{r}_e|e|$ for all $\theta\in[0,1]$, then

$$|\mathbf{J}(s,\theta)| \leq |e| + \frac{\ell(\theta)}{\alpha(\theta)}(|\mathbf{m}^{\mathbf{u}}| + |\mathbf{m}^{\mathbf{v}}|) \leq |e| + 2\sqrt{2}\,\gamma_{K^e}\widetilde{r}_e|e|.$$

Thus,

$$\|\mathbf{p}\|^2_{0,\widetilde{K}^e_{ext}} \leq \left(1+2\sqrt{2}\,\gamma_{K^e}\widetilde{r}_e\right)|e|\int_0^1\int_0^{\ell(\theta)}|\mathbf{p}(\mathbf{y}(s,\theta))|^2\,ds\,d\theta = \left(1+2\sqrt{2}\,\gamma_{K^e}\widetilde{r}_e\right)|\!|\!|\mathbf{p}|\!|\!|^2_e,$$

which implies (3.16).

On the other hand, we notice that the Jacobian (3.14) can be written as

$$\mathbf{J}(s,\theta) = \left|\,|e|\mathbf{m}(\theta)\cdot\boldsymbol{\nu}_e + \frac{s}{\alpha(\theta)}\mathbf{m}^{\mathbf{u}}\cdot(\mathbf{m}^{\mathbf{v}})^{\perp}\right|. \tag{3.18}$$

Then, by assumptions (ii) and (iii), we have that $\mathbf{J}(s,\theta)\geq\beta_e|e|$. Thus, by (3.15) we obtain (3.17). ■

Then we have the following intermediate result.

Lemma 3.5. *In addition to the hypotheses of Theorem 2.2 and assumption (i) in Lemma 3.4, we suppose that there exists an integer $m\geq 0$ such that $\boldsymbol{\sigma}\in\mathbf{H}^{m+1}(\Omega)$. Then, for any $\boldsymbol{\zeta}_h\in\mathbf{H}_h(\mathrm{D}_h)$, there hold*

$$\sum_{e\in\mathcal{E}_h^\partial}\|\boldsymbol{\sigma}-\mathbf{E}_h(\boldsymbol{\zeta}_h)\|_{0,\widetilde{K}^e_{ext}} \lesssim h^{m+1}\|\boldsymbol{\sigma}\|_{m+1,\Omega} + \|\boldsymbol{\sigma}-\boldsymbol{\zeta}_h\|_{0,\mathrm{D}_h} \tag{3.19}$$

and

$$\sum_{e\in\mathcal{E}_h^\partial}\|\boldsymbol{\sigma}-\mathbf{E}_h(\boldsymbol{\zeta}_h)\|_{\mathrm{div}\,;\widetilde{K}^e_{ext}} \lesssim \|\boldsymbol{\sigma}-\boldsymbol{\zeta}_h\|_{\mathrm{div}\,;\mathrm{D}_h} + h^{m+1}\Big(\|\boldsymbol{\sigma}\|_{m+1,\Omega} + \|\mathrm{div}\,\boldsymbol{\sigma}\|_{m+1,\Omega}\Big). \tag{3.20}$$

Proof. Let $\boldsymbol{\zeta}_h\in\mathbf{H}_h(\mathrm{D}_h)$ and $\mathscr{E}:\mathrm{H}^{m+1}(\Omega)\to\mathrm{H}^{m+1}(\mathbb{R}^2)$ be the extension operator introduced in Theorem 2.1. Then, since Γ is Lipschitz (cf. assumption (A.1)), we define

$$\boldsymbol{\psi}_e := (\mathrm{T}_e^{m+1}(\mathscr{E}\sigma_1), \mathrm{T}_e^{m+1}(\mathscr{E}\sigma_2))^{\mathtt{t}}, \tag{3.21}$$

where, for each $i\in\{1,2\}$ and for any $e\in\mathcal{E}_h^\partial$, $\mathrm{T}_e^{m+1}(\mathscr{E}\sigma_i)$ is the Taylor polynomial of degree $m+1$ of the function $\mathscr{E}\sigma_i$ around the center of the ball $\widetilde{B}^e$ (see [6, Chapter IV] for details), with $\widetilde{B}^e$ being the ball of radius $h_{\widetilde{B}^e}$ (equal to the diameter of $\widetilde{K}^e_{ext}\cup K^e$) centered at the middle point of the edge e; see Figure 4. Thus, by definition, $\boldsymbol{\psi}_e\in\mathbf{P}_s(\widetilde{B}^e)$ with $s<m+1$.

Then, by triangle inequality, definition (2.14) and Lemma 3.4, we obtain

$$\begin{aligned}\|\boldsymbol{\sigma}-\mathbf{E}_h(\boldsymbol{\zeta}_h)\|_{0,\widetilde{K}^e_{ext}} &\leq \|\boldsymbol{\sigma}-\boldsymbol{\psi}_e\|_{0,\widetilde{K}^e_{ext}} + \|\boldsymbol{\psi}_e-\mathbf{E}_h(\boldsymbol{\zeta}_h)\|_{0,\widetilde{K}^e_{ext}}\\ &\leq \|\boldsymbol{\sigma}-\boldsymbol{\psi}_e\|_{0,\widetilde{K}^e_{ext}} + C_2^e\widetilde{r}_e^{1/2}\widetilde{C}^e_{ext}\|\boldsymbol{\psi}_e-\boldsymbol{\zeta}_h\|_{0,K^e}\\ &\leq \left(1+C_2^e\widetilde{r}_e^{1/2}\widetilde{C}^e_{ext}\right)\|\boldsymbol{\sigma}-\boldsymbol{\psi}_e\|_{0,\widetilde{K}^e_{ext}} + C_2^e\widetilde{r}_e^{1/2}\widetilde{C}^e_{ext}\|\boldsymbol{\sigma}-\boldsymbol{\zeta}_h\|_{0,K^e},\end{aligned} \tag{3.22}$$

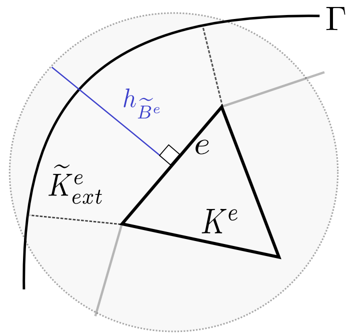

Figure 4: Example of the ball $\widetilde{B}^e$ associated with the boundary edge e.

where in the last inequality we added and subtracted $\boldsymbol{\sigma}$. On the other hand, by approximations properties of the Taylor polynomials (cf. Section 4.1 in [6]), we have

$$\|\boldsymbol{\sigma} - \boldsymbol{\psi}_e\|_{0,\widetilde{K}^e_{ext}} \leq h^{m+1} |\boldsymbol{\mathscr{E}}\boldsymbol{\sigma}|_{m+1,\widetilde{B}^e}, \tag{3.23}$$

where $\boldsymbol{\mathscr{E}}\boldsymbol{\sigma} := (\mathscr{E}\sigma_1, \mathscr{E}\sigma_2)^{\mathsf{t}}$. Thus, replacing (3.23) in (3.22), adding over $e \in \mathcal{E}_h^\partial$, using the continuity of $\boldsymbol{\mathscr{E}}$ and Assumptions in $\mathbf{D}$, we obtain (3.19).

On the other hand, we notice that $\operatorname{div} \mathbf{E}_h(\boldsymbol{\zeta}_h)(\mathbf{y}) = \mathbf{E}_h(\operatorname{div} \boldsymbol{\zeta}_h)(\mathbf{y})$ for all $\mathbf{y} \in \widetilde{K}^e_{ext}$. Then, repeating the arguments that led us to (3.19), but this time taking $w_e := \mathrm{T}_e^m(\mathscr{E}(\operatorname{div} \boldsymbol{\sigma})) \in \mathrm{P}_s(\widetilde{B}^e)$, with $s < m$, instead of $\boldsymbol{\psi}_e$, we readily deduce that

$$\begin{aligned}\sum_{e \in \mathcal{E}_h^\partial} \|\operatorname{div} \boldsymbol{\sigma} - \operatorname{div} \mathbf{E}_h(\boldsymbol{\zeta}_h)\|_{0,\widetilde{K}^e_{ext}} &\leq \sum_{e \in \mathcal{E}_h^\partial} \left\{ \|\operatorname{div} \boldsymbol{\sigma} - w_e\|_{0,\widetilde{K}^e_{ext}} + \|\operatorname{div} \mathbf{E}_h(\boldsymbol{\zeta}_h) - w_e\|_{0,\widetilde{K}^e_{ext}} \right\} \\ &\lesssim h^{m+1} \|\operatorname{div} \boldsymbol{\sigma}\|_{m+1,\Omega} + \|\operatorname{div}(\boldsymbol{\sigma} - \boldsymbol{\zeta}_h)\|_{0,\mathrm{D}_h},\end{aligned}$$

which together with (3.19) implies (3.20). ■

We now propose suitable approximations for $\boldsymbol{\sigma}$ and u in D_h^c. These approximations, in abuse of notation, we will be named also $\boldsymbol{\sigma}_h$ and u_h. To that end we let $(\boldsymbol{\sigma}_h, u_h) \in \mathbf{H}_h(\mathrm{D}_h) \times \mathrm{Q}_h(\mathrm{D}_h)$ be the unique solution of (2.11).

First, to approximate $\boldsymbol{\sigma}$ in D_h^c, we proceed analogously to [17, Section 2.1.3] and simply take the extrapolation of $\boldsymbol{\sigma}_h$ in D_h^c, that is, for any $e \in \mathcal{E}_h^\partial$ and any $\mathbf{y} \in \widetilde{K}^e_{ext}$, we define

$$\boldsymbol{\sigma}_h(\mathbf{y}) := \mathbf{E}_h(\boldsymbol{\sigma}_h)(\mathbf{y}). \tag{3.24}$$

Observe that, for each edge $e \in \mathcal{E}_h^\partial$, the extrapolation of $\boldsymbol{\sigma}_h|_{K^e}$ to $\widetilde{K}^e_{ext}$ belongs to $\mathbf{H}(\operatorname{div}; \widetilde{K}^e_{ext})$, but not necessarily to $\mathbf{H}(\operatorname{div}; \mathrm{D}_h^c)$. Consequently, for the subsequent analysis we introduce the broken space (see for instance [12]):

$$\mathbf{H}(\operatorname{div}; \widetilde{\mathrm{T}}_h) := \prod_{e \in \mathcal{E}_h^\partial} \mathbf{H}(\operatorname{div}; \widetilde{K}^e_{ext})$$

endowed with the broken norm

$$\|\boldsymbol{\xi}\|_{\operatorname{div};\widetilde{\mathrm{T}}_h} := \left\{ \sum_{e \in \mathcal{E}_h^\partial} \|\boldsymbol{\xi}\|^2_{\operatorname{div};\widetilde{K}^e_{ext}} \right\}^{1/2}.$$

The following result establishes the estimate for $\boldsymbol{\sigma} - \boldsymbol{\sigma}_h$ in D_h^c.

Lemma 3.6. *Suppose that assumptions of Lemma 3.5 are satisfied. Then*

$$\begin{aligned}\|\boldsymbol{\sigma}-\boldsymbol{\sigma}_h\|_{\mathrm{div};\widetilde{\mathrm{T}}_h} \lesssim & \inf_{\boldsymbol{\zeta}_h\in\mathbf{H}_h(\mathrm{D}_h)}\|\boldsymbol{\sigma}-\boldsymbol{\zeta}_h\|_{\mathrm{div};\mathrm{D}_h} + \inf_{w_h\in\mathrm{Q}_h(\mathrm{D}_h)}\|u-w_h\|_{0,\mathrm{D}_h} \\ & +\|\boldsymbol{\sigma}-\boldsymbol{\sigma}_h\|_{\mathrm{div};\mathrm{D}_h} + h^{m+1}\Big(\|\boldsymbol{\sigma}\|_{m+1,\Omega}+\|\mathrm{div}\,\boldsymbol{\sigma}\|_{m+1,\Omega}\Big)\end{aligned} \tag{3.25}$$

and

$$\begin{aligned}\|\boldsymbol{\sigma}-\boldsymbol{\sigma}_h\|_{0,\mathrm{D}_h^c} \lesssim & \inf_{\boldsymbol{\zeta}_h\in\mathbf{H}_h(\mathrm{D}_h)}\|\boldsymbol{\sigma}-\boldsymbol{\zeta}_h\|_{0,\mathrm{D}_h^c} + \inf_{w_h\in\mathrm{Q}_h(\mathrm{D}_h)}\|u-w_h\|_{0,\mathrm{D}_h} \\ & +\|\boldsymbol{\sigma}-\boldsymbol{\sigma}_h\|_{0,\mathrm{D}_h} + h^{m+1}\|\boldsymbol{\sigma}\|_{m+1,\Omega}.\end{aligned} \tag{3.26}$$

Proof. Let $\boldsymbol{\zeta}_h\in\mathbf{H}_h(\mathrm{D}_h)$. By applying estimate (3.20), we deduce that

$$\begin{aligned}\|\boldsymbol{\sigma}-\boldsymbol{\sigma}_h\|_{\mathrm{div};\widetilde{\mathrm{T}}_h} &\leq \sum_{e\in\mathcal{E}_h^\partial}\|\boldsymbol{\sigma}-\boldsymbol{\sigma}_h\|_{\mathrm{div};\widetilde{K}^e_{ext}} \\ &\lesssim \|\boldsymbol{\zeta}_h-\boldsymbol{\sigma}_h\|_{\mathrm{div};\mathrm{D}_h}+\|\boldsymbol{\sigma}-\boldsymbol{\zeta}_h\|_{\mathrm{div};\mathrm{D}_h}+h^{m+1}\Big(\|\boldsymbol{\sigma}\|_{m+1,\Omega}+\|\mathrm{div}\,\boldsymbol{\sigma}\|_{m+1,\Omega}\Big),\end{aligned}$$

Hence, adding an subtracting $\boldsymbol{\sigma}$ in $\|\boldsymbol{\zeta}_h-\boldsymbol{\sigma}_h\|_{\mathrm{div};\mathrm{D}_h}$ we obtain (3.25). In addition, (3.26) is obtained analogously, but considering the estimate (3.19) instead of (3.20). ■

Now, to define the approximation of u in D_h^c, we proceed again analogously to [17, Section 2.1.3] and adopt the same ideas when defining $\widetilde{g}_h$ (cf. (2.8)). More precisely, given an edge $e\in\mathcal{E}_h^\partial$, for any point $\mathbf{y}\in\widetilde{K}^e_{ext}$ there is a path $\mathscr{C}(\mathbf{x})$ starting at $\mathbf{x}\in\Gamma_h$ and ending at $\widetilde{\mathbf{x}}\in\Gamma$ so that we can write $\mathbf{y}=\mathbf{x}+(\eta/\ell(\mathbf{x}))(\widetilde{\mathbf{x}}-\mathbf{x})$ for some $\eta\in[0,\ell(\mathbf{x})]$. Then, for any $e\in\mathcal{E}_h^\partial$ and $\mathbf{y}\in\widetilde{K}^e_{ext}$, we set

$$u_h(\mathbf{y}) := u(\widetilde{\mathbf{y}}) - \int_0^{|\widetilde{\mathbf{y}}-\mathbf{y}|}\boldsymbol{\sigma}_h(\mathbf{y}+s\mathbf{w}(\mathbf{y}))\cdot\mathbf{w}(\mathbf{y})ds, \tag{3.27}$$

where $\widetilde{\mathbf{y}}:=\widetilde{\mathbf{x}}$, $\mathbf{w}(\mathbf{y}):=(\widetilde{\mathbf{y}}-\mathbf{y})/|\widetilde{\mathbf{y}}-\mathbf{y}|$ and $\boldsymbol{\sigma}_h$ is defined as in (3.24).

Now we address the estimate for $u-u_h$ by using the L^2-norm on D_h^c.

Lemma 3.7. *Suppose that assumptions of Lemmas 3.4 and 3.5 are satisfied, then*

$$\|u-u_h\|_{0,\mathrm{D}_h^c} \lesssim \quad h^{m+2}\|\boldsymbol{\sigma}\|_{m+1,\Omega} + h\left(\inf_{w_h\in\mathrm{Q}_h(\mathrm{D}_h)}\|u-w_h\|_{0,\mathrm{D}_h} + \inf_{\boldsymbol{\zeta}_h\in\mathbf{H}_h(\mathrm{D}_h)}\|\boldsymbol{\sigma}-\boldsymbol{\zeta}_h\|_{\mathrm{div};\mathrm{D}_h}\right).$$

Proof. We first use (3.16) to obtain

$$\|u-u_h\|^2_{0,\mathrm{D}_h^c} \leq \sum_{e\in\mathcal{E}_h^\partial}(C_2^e)^2\,|||u-u_h|||_e^2 = \sum_{e\in\mathcal{E}_h^\partial}(C_2^e)^2\int_e\int_0^{\ell(\mathbf{x})}|u-u_h|^2(\mathbf{x}+t\mathbf{m}(\mathbf{x}))\,dt\,dS_{\mathbf{x}}. \tag{3.28}$$

Let $\mathbf{y}=\mathbf{x}+t\mathbf{m}(\mathbf{x})$, then using the definition of $u_h(\mathbf{y})$ in (3.27) and the facts that $\widetilde{\mathbf{y}}=\widetilde{\mathbf{x}}$ and $\mathbf{w}(\mathbf{y})=\mathbf{m}(\mathbf{x})$, we have

$$\begin{aligned}(u-u_h)(\mathbf{y}) &= -\int_0^{|\widetilde{\mathbf{y}}-\mathbf{y}|}(\boldsymbol{\sigma}-\boldsymbol{\sigma}_h)(\mathbf{y}+s\mathbf{w}(\mathbf{y}))\cdot\mathbf{w}(\mathbf{y})\,ds \\ &= -\int_0^{(\ell(\mathbf{x})-t)}(\boldsymbol{\sigma}-\boldsymbol{\sigma}_h)(\mathbf{x}+(t+s)\mathbf{m}(\mathbf{x}))\cdot\mathbf{m}(\mathbf{x})\,ds.\end{aligned}$$

This expression, together with the Cauchy–Schwarz inequality and a simple change of variables, implies

$$\begin{aligned}|u-u_h|^2(\mathbf{y}) &\leq (\ell(\mathbf{x})-t)\int_t^{\ell(\mathbf{x})} |(\boldsymbol{\sigma}-\boldsymbol{\sigma}_h)(\mathbf{x}+r\mathbf{m}(\mathbf{x}))|^2\,dr \\ &\leq \ell(\mathbf{x})\int_0^{\ell(\mathbf{x})} |(\boldsymbol{\sigma}-\boldsymbol{\sigma}_h)(\mathbf{x}+r\mathbf{m}(\mathbf{x}))|^2\,dr.\end{aligned}\tag{3.29}$$

In this way, replacing (3.29) into (3.28), we obtain

$$\|u-u_h\|_{0,\mathrm{D}_h^c}^2 \leq \sum_{e\in\mathcal{E}_h^\partial} (C_2^e)^2 \int_e \ell(\mathbf{x})^2 \int_0^{\ell(\mathbf{x})} |(\boldsymbol{\sigma}-\boldsymbol{\sigma}_h)(\mathbf{x}+r\mathbf{m}(\mathbf{x}))|^2\,dr. \tag{3.30}$$

Since $\ell(\mathbf{x})\leq \widetilde{H}_e=\widetilde{r}_e h_e^\perp \leq \widetilde{r}_e h_{K^e}$, thanks to assumption (D.1) and (3.17), we obtain

$$\|u-u_h\|_{0,\mathrm{D}_h^c}^2 \leq \sum_{e\in\mathcal{E}_h^\partial} (C_2^e)^2\,\widetilde{r}_e h_{K^e} |||\boldsymbol{\sigma}-\boldsymbol{\sigma}_h|||_e^2 \leq (Rh)^2 \max_{e\in\mathcal{E}_h^\partial} (C_2^e)^2\,(C_1^e)^{-2}\|\boldsymbol{\sigma}-\boldsymbol{\sigma}_h\|_{0,\mathrm{D}_h^c}^2.$$

and the result follows from (3.26). ■

Remark 3.1. *The solvability and error analyses in previous sections do not rely on how the computational subdomain and the transferring paths are constructed, as long as Assumptions* **A**, **D** *and assumptions of Lemma 3.4 are satisfied.*

Remark 3.2. *We now illustrate an alternative way to construct the computational domain D_h. If Ω is convex, we can construct Γ_h interpolating Γ by a piecewise linear function. Thus, the subdomain D_h is the region enclosed by Γ_h and the transferring paths associated to the interior points of a boundary edge e can be chosen so that they are perpendicular to e. In this setting, Assumptions* **A** *and* **D** *hold and actually $\widetilde{r}_e$ is of order h. Moreover, the norms $\|\cdot\|_{0,\widetilde{K}_{ext}^e}$ and $|||\cdot|||$ coincide and hence Assumptions $(i)-(iii)$ of Lemma 3.4 are not necessary. If Ω is not convex, we can proceed similarly and our analysis still holds under the additional assumption that the solution $(\boldsymbol{\sigma},u)$ of (2.1) can be extended to the region $\Omega^c\cap\mathrm{D}_h$.*

4 Particular choice of finite elements

Given an integer $k\geq 0$ and a set $\mathcal{O}$ in $\mathbb{R}^2$, we denote by $\widetilde{\mathrm{P}}_k(\mathcal{O})\subset\mathrm{P}_k(\mathcal{O})$ the space of polynomials of total degree equal to k. Then, with the same notations and definitions introduced in Section 2.1 concerning the triangulation T_h of $\overline{\mathrm{D}_h}$, we start by defining the local Raviart–Thomas space of order k as

$$\mathbf{RT}_k(K) := \mathbf{P}_k(K)\oplus\widetilde{\mathrm{P}}_k(K)\mathbf{x},$$

or each $K\in\mathrm{T}_h$, where $\mathbf{x}:=(x_1,x_2)^{\mathbf{t}}$ is a generic vector of $\mathbb{R}^2$, and $\mathbf{P}_k(K)$ stands for the space of vector-valued polynomials of degree at most k on $K\in\mathrm{T}_h$. Then, a concrete example of discrete spaces for is given by the sets:

$$\begin{aligned}\mathbf{H}_h(\mathrm{D}_h) &:= \left\{\boldsymbol{\tau}_h\in\mathbf{H}(\mathrm{div}\,;\mathrm{D}_h):\ \boldsymbol{\tau}_h\big|_K\in\mathbf{RT}_k(K)\quad\forall\,K\in\mathrm{T}_h\right\},\\ \mathrm{Q}_h(\mathrm{D}_h) &:= \left\{v_h\in\mathrm{L}^2(\mathrm{D}_h):\ v_h\big|_K\in\mathrm{P}_k(K)\quad\forall\,K\in\mathrm{T}_h\right\}.\end{aligned}\tag{4.1}$$

It is well-known that these spaces satisfy assumptions **B** and **C** (cf. Section 2.4). Moreover, they have the following approximation properties (see, e.g. [21, 24]):

$(\mathbf{AP}_h^{\boldsymbol{\sigma}})$ For each $r \in (0, k+1]$, and for each $\boldsymbol{\sigma} \in \mathbf{H}^r(\mathrm{D}_h) \cap \mathbf{H}(\mathrm{div}\,; \mathrm{D}_h)$ with $\mathrm{div}\,\boldsymbol{\sigma} \in \mathrm{H}^r(\mathrm{D}_h)$, there holds

$$\inf_{\boldsymbol{\zeta}_h \in \mathbf{H}_h(\mathrm{D}_h)} \|\boldsymbol{\sigma} - \boldsymbol{\zeta}_h\|_{\mathrm{div}\,;\mathrm{D}_h} \lesssim h^r \Big(\|\boldsymbol{\sigma}\|_{r,\mathrm{D}_h} + \|\mathrm{div}\,\boldsymbol{\sigma}\|_{r,\mathrm{D}_h} \Big).$$

$(\mathbf{AP}_h^{u})$ For each $r \in (0, k+1]$, and for each $u \in \mathrm{H}^r(\mathrm{D}_h)$, there holds

$$\inf_{w_h \in \mathrm{Q}_h(\mathrm{D}_h)} \|u - w_h\|_{0,\mathrm{D}_h} \lesssim h^r \|u\|_{r,\mathrm{D}_h}.$$

The following theorem establishes the *a priori* error estimates associated to the scheme (2.4), under suitable regularity assumptions on the exact solution. It also provides estimates of the error in the non-meshed region D_h^c.

Theorem 4.1. *In addition to the hypotheses of Theorem 3.3, Lemma, Lemma 3.4 and 3.5, let us assume that the exact solution* $(\boldsymbol{\sigma}, u)$ *satisfies* $\boldsymbol{\sigma} \in \mathbf{H}^{k+1}(\Omega) \cap \mathbf{H}(\mathrm{div}\,;\Omega)$ *with* $\mathrm{div}\,\boldsymbol{\sigma} \in \mathrm{H}^{k+1}(\Omega)$ *and* $u \in \mathrm{H}^{k+1}(\Omega)$*. Then*

$$\|(\boldsymbol{\sigma}, u) - (\boldsymbol{\sigma}_h, u_h)\|_{\mathbf{H}(\mathrm{div}\,;\mathrm{D}_h)\times \mathrm{L}^2(\mathrm{D}_h)} \lesssim h^{k+1}\Big(\|\boldsymbol{\sigma}\|_{k+1,\Omega} + \|\mathrm{div}\,\boldsymbol{\sigma}\|_{k+1,\Omega} + \|u\|_{k+1,\Omega}\Big),$$

$$\|\boldsymbol{\sigma} - \mathbf{E}_h(\boldsymbol{\sigma}_h)\|_{\mathrm{div}\,;\widetilde{\mathrm{T}}_h} \lesssim h^{k+1}\Big(\|\boldsymbol{\sigma}\|_{k+1,\Omega} + \|\mathrm{div}\,\boldsymbol{\sigma}\|_{k+1,\Omega} + \|u\|_{k+1,\Omega}\Big),$$

and

$$\|u - u_h\|_{0,\mathrm{D}_h^c} \lesssim h^{k+2}\Big(\|\boldsymbol{\sigma}\|_{k+1,\Omega} + \|\mathrm{div}\,\boldsymbol{\sigma}\|_{k+1,\Omega} + \|u\|_{k+1,\Omega}\Big).$$

Proof. It follows from Theorem 3.3, Lemmas 3.6, 3.7, and the approximations properties $(\mathbf{AP}_h^{u})$ and $(\mathbf{AP}_h^{\boldsymbol{\sigma}})$ specified above. ■

Remark 4.1. *The theory developed above covers other similar finite element subspaces available in the literature, such as the local Brezzi–Douglas–Marini space of order* $k \geq 1$ *(see for instance [9]):*

$$\mathbf{BDM}_k(K) := \mathbf{P}_k(K).$$

More precisely, one can also choose the discrete spaces in (2.7) *as:*

$$\begin{aligned}\mathbf{H}_h(\mathrm{D}_h) &:= \Big\{ \boldsymbol{\tau}_h \in \mathbf{H}(\mathrm{div}\,;\mathrm{D}_h) :\ \boldsymbol{\tau}_h\big|_K \in \mathbf{BDM}_k(K) \quad \forall\, K \in \mathrm{T}_h \Big\},\\ \mathrm{Q}_h(\mathrm{D}_h) &:= \Big\{ v_h \in \mathrm{L}^2(\mathrm{D}_h) :\ v_h\big|_K \in \mathrm{P}_{k-1}(K) \quad \forall\, K \in \mathrm{T}_h \Big\},\end{aligned}$$

and obtain the well–posedness of the discrete problem and optimal error estimates, as well.

5 Numerical results

In this section we present numerical experiments in $\mathbb{R}^2$ illustrating the performance of the discrete scheme introduced and analized in Section 2. The numerical results shown below were obtained using a `MATLAB` code, along with the direct linear solver `UMFPACK` (cf. [19]), also incorporated as a built-in function into `MATLAB`. In all the computations we consider the specific finite element subspaces $\mathbf{H}_h(\mathrm{D}_h)$ and $\mathrm{Q}_h(\mathrm{D}_h)$ defined in terms of the discrete spaces given by (4.1) with $k = 0, 1, 2, 3$. At this regard, an important issue is the computational implementation of specific basis functions providing high order approximations. This is facilitated through the use of *hierarchical* basis for the local Raviart–Thomas space of order k, as was introduced in [1], and Dubiner basis for the local polynomial space of degree at most k (see e.g. [20]). We begin by introducing additional notations. Firstly, we must take into account that, in all our examples, the computational domain D_h and the region D_h^c change with h. That is why we compute the relative errors

$$\mathsf{e}_{\mathtt{int}}(u) := \frac{\|u - u_h\|_{0,\mathrm{D}_h}}{\|u\|_{0,\mathrm{D}_h}}, \quad \mathsf{e}_{\mathtt{int}}(\boldsymbol{\sigma}) := \frac{\|\boldsymbol{\sigma} - \boldsymbol{\sigma}_h\|_{\mathrm{div}\,;\mathrm{D}_h}}{\|\boldsymbol{\sigma}\|_{\mathrm{div}\,;\mathrm{D}_h}},$$
$$\mathsf{e}_{\mathtt{ext}}(u) := \frac{\|u - u_h\|_{0,\mathrm{D}_h^c}}{\|u\|_{0,\mathrm{D}_h^c}}, \quad \mathsf{e}_{\mathtt{ext}}(\boldsymbol{\sigma}) := \frac{\|\boldsymbol{\sigma} - \mathbf{E}_h(\boldsymbol{\sigma}_h)\|_{\mathrm{div}\,;\widetilde{\mathrm{T}}_h}}{\|\boldsymbol{\sigma}\|_{\mathrm{div}\,;\widetilde{\mathrm{T}}_h}}.$$

Subsequently, we define the experimental rates of convergence as

$$\mathsf{r}_{\mathtt{int}}(\cdot) := -2\left\{\frac{\log(\mathsf{e}_{\mathtt{int}}(\cdot)/\mathsf{e'}_{\mathtt{int}}(\cdot))}{\log(N/N')}\right\}, \quad \mathsf{r}_{\mathtt{ext}}(\cdot) := -2\left\{\frac{\log(\mathsf{e}_{\mathtt{ext}}(\cdot)/\mathsf{e'}_{\mathtt{ext}}(\cdot))}{\log(N/N')}\right\},$$

where N and N' denote the number of elements of two consecutive meshes with their respective errors $\mathsf{e}_{\mathtt{int}}$ and $\mathsf{e}'_{\mathtt{int}}$ (resp. $\mathsf{e}_{\mathtt{ext}}$ and $\mathsf{e}'_{\mathtt{ext}}$).

Example 1. We take $u(x_1, x_2) := \sin(\pi x_1)\sin(\pi x_2)$ as exact solution, and choose Ω to be the *annular* domain consisting in two concentric circles of radius 1.5 and 0.7, respectively. As required by assumption (D.1), the subdomain D_h is constructed in such a way that the distance $d(\Gamma, \Gamma_h)$ is at most $\mathcal{O}(h)$. To do that, we consider a background triangulation $\mathcal{T}_h$ of the square $\mathcal{B} \supset \Omega$, obtained by subdividing the squares of the Cartesian grid into four congruent triangles, and then follow the process in Section 2.1 to choose those elements of $\mathcal{T}_h$ inside of Ω. In Table 1 we present the history of convergence and observe that the convergence rates predicted by Theorem 4.1 are attained by all the unknowns, namely $\mathcal{O}(h^{k+1})$ for $\mathsf{e}_{\mathtt{int}}(\boldsymbol{\sigma})$, $\mathsf{e}_{\mathtt{ext}}(\boldsymbol{\sigma})$ and $\mathsf{e}_{\mathtt{int}}(u)$, and $\mathcal{O}(h^{k+2})$ for $\mathsf{e}_{\mathtt{ext}}(u)$. Next, in Figure 5 we display the approximate value of the second component of $\boldsymbol{\sigma}$, denoted by $\sigma_{h,2}$, obtained for the approximation $\mathbf{RT}_3 - \mathrm{P}_3$ with total number of degrees of freedom (d.o.f) equal to 32560 and $N = 1152$ elements. The corresponding extrapolated solution on the set D_h^c is also displayed there.

Example 2. We set f and g such that $u(x_1, x_2) := x_1^2 \exp(2(x_2 - 1))$, and consider a *kidney-shaped* domain Ω whose boundary satisfies the equation

$$(2[(x_1 + 0.5)^2 + x_2^2] - x_1 - 0.5)^2 - [(x_1 + 0.5)^2 + x_2^2] + 0.1 = 0.$$

The way to construct D_h is the same as in the previous example. In Table 2 we present the corresponding convergence history and again observe there that optimal convergence rates predicted by Theorem 4.1 are reached by all the unknowns. In Figure 6 we display the approximate value of the first component of $\boldsymbol{\sigma}$, denoted by $\sigma_{h,1}$, obtained for the approximation $\mathbf{RT}_3 - \mathrm{P}_3$ with total number of degrees of freedom (d.o.f) equal to 18480 and $N = 654$ elements.

Example 3. We consider exactly the same domain Ω as in Example 2, but this time we choose $u(x_1, x_2) := \sin(10\pi x_1 - 5\pi x_2)$ as exact solution instead. The goal is to explore how the error of our method is affected when we consider keeping a triangulation of $\overline{\mathrm{D}_h}$ fixed and varying the degree k of the finite element spaces in (4.1). In Figure 7 we show the results for three fixed meshes with $N = 146$, $N = 654$ and $N = 3068$ elements, respectively. As expected, it can be appreciated there that the quality of the approximations improves as h diminishes or k increases.

Example 4. In our last experiment, we observe the performance of the method considering another type of computational domain, as Remark 3.2 mentioned. We take $u(x_1, x_2) := \sin(x_1)\sin(x_2)$ as exact solution and consider Ω to be the annular domain consisting of two concentric circles of radius

				Errors on D_h				Errors on D_h^c			
k	N	h	d.o.f	$\mathsf{e}_{\mathtt{int}}(u)$	$\mathsf{r}_{\mathtt{int}}(u)$	$\mathsf{e}_{\mathtt{int}}(\boldsymbol{\sigma})$	$\mathsf{r}_{\mathtt{int}}(\boldsymbol{\sigma})$	$\mathsf{e}_{\mathtt{ext}}(u)$	$\mathsf{r}_{\mathtt{ext}}(u)$	$\mathsf{e}_{\mathtt{ext}}(\boldsymbol{\sigma})$	$\mathsf{r}_{\mathtt{ext}}(\boldsymbol{\sigma})$
0	248	0.262	664	$2.28e-01$	–	$2.30e-01$	–	$9.84e-03$	–	$2.99e-01$	–
	1152	0.131	2956	$1.08e-01$	0.96	$1.10e-01$	0.96	$2.28e-03$	1.90	$1.24e-01$	1.14
	4840	0.065	12260	$5.31e-02$	0.99	$5.39e-02$	0.99	$5.52e-04$	1.97	$6.50e-02$	0.90
	22028	0.031	55352	$2.20e-02$	1.16	$2.26e-02$	1.14	$1.62e-04$	1.61	$3.28e-02$	0.90
	89384	0.015	224020	$1.09e-02$	0.99	$1.12e-02$	0.99	$3.22e-05$	2.30	$1.58e-02$	1.03
1	248	0.262	2072	$2.79e-02$	–	$2.37e-02$	–	$3.62e-03$	–	$1.08e-01$	–
	1152	0.131	9368	$5.44e-03$	2.13	$5.51e-03$	1.90	$4.72e-04$	2.65	$2.43e-02$	1.94
	4840	0.065	39040	$1.32e-03$	1.96	$1.36e-03$	1.95	$5.35e-05$	3.03	$6.70e-03$	1.79
	22028	0.031	176790	$2.95e-04$	1.97	$3.03e-04$	1.97	$5.02e-06$	3.12	$1.79e-03$	1.74
	89384	0.015	716200	$7.36e-05$	1.98	$7.56e-05$	1.98	$5.86e-07$	3.06	$4.41e-04$	1.99
2	248	0.262	4224	$6.51e-03$	–	$2.88e-03$	–	$9.75e-04$	–	$2.16e-02$	5.87
	1152	0.131	19236	$2.74e-04$	4.12	$2.58e-04$	3.14	$4.57e-05$	3.98	$1.76e-03$	3.26
	4840	0.065	80340	$3.01e-05$	3.07	$3.13e-05$	2.93	$4.51e-06$	3.22	$2.97e-04$	2.48
	22028	0.031	364310	$2.32e-06$	3.38	$2.42e-06$	3.37	$1.18e-07$	4.80	$2.53e-05$	3.24
	89384	0.015	1476500	$2.84e-07$	2.99	$2.96e-07$	3.00	$7.08e-09$	4.02	$2.92e-06$	3.08
3	248	0.262	7120	$2.27e-03$	–	$7.27e-04$	–	$2.25e-04$	–	$5.59e-03$	–
	1152	0.131	32560	$2.83e-05$	5.70	$1.70e-05$	4.88	$3.48e-06$	5.43	$2.82e-04$	3.88
	4840	0.065	136160	$1.16e-06$	4.44	$1.22e-06$	3.67	$2.25e-07$	3.81	$2.56e-05$	3.34
	22028	0.031	617910	$1.67e-08$	5.59	$2.18e-08$	5.31	$1.72e-09$	6.43	$1.52e-06$	3.72
	89384	0.015	2505000	$9.51e-10$	4.09	$1.14e-09$	4.20	$4.27e-11$	5.28	$8.87e-08$	4.05

Table 1: History of convergence of the approximation in Example 1.

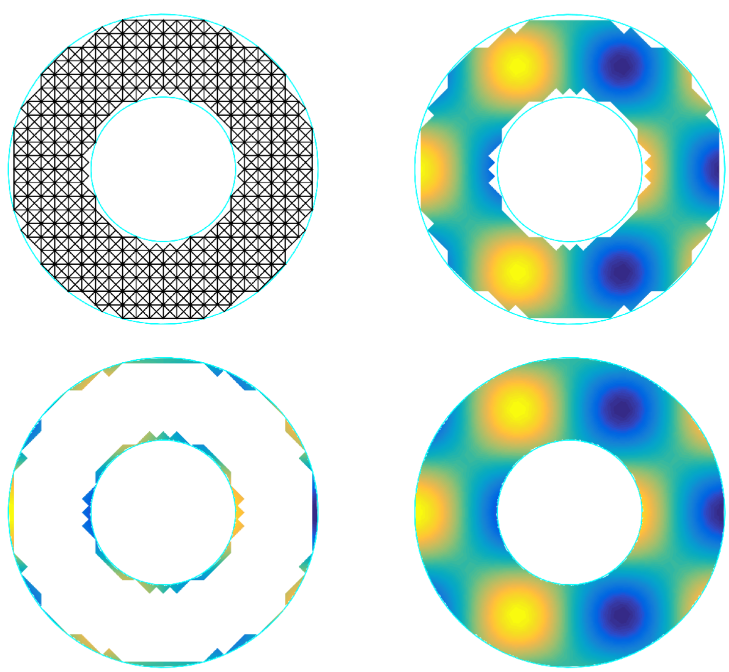

Figure 5: Example 1: $\sigma_{h,2}$ for the approximation $\mathbf{RT}_3 - \mathrm{P}_3$ with $N = 1152$ elements.

				Errors on D_h				Errors on D_h^c			
k	N	h	d.o.f	$\mathtt{e_{int}}(u)$	$\mathtt{r_{int}}(u)$	$\mathtt{e_{int}}(\boldsymbol{\sigma})$	$\mathtt{r_{int}}(\boldsymbol{\sigma})$	$\mathtt{e_{ext}}(u)$	$\mathtt{r_{ext}}(u)$	$\mathtt{e_{ext}}(\boldsymbol{\sigma})$	$\mathtt{r_{ext}}(\boldsymbol{\sigma})$
0	146	0.131	384	$1.65e-01$	–	$5.12e-02$	–	$3.51e-03$	–	$1.01e-01$	–
	654	0.065	1677	$7.88e-02$	0.98	$2.61e-02$	0.89	$1.51e-03$	1.12	$5.25e-02$	0.88
	3068	0.031	7748	$3.84e-02$	0.93	$1.12e-02$	1.09	$2.91e-04$	2.13	$2.63e-02$	0.89
	12579	0.015	31602	$1.89e-02$	0.99	$5.64e-03$	0.97	$7.13e-05$	1.99	$1.32e-02$	0.96
	50877	0.007	127500	$9.44e-03$	0.99	$2.82e-03$	0.98	$1.66e-05$	2.08	$6.68e-03$	0.98
1	146	0.131	1206	$1.22e-02$	–	$2.19e-03$	–	$4.48e-04$	–	$8.88e-03$	–
	654	0.065	5316	$2.68e-03$	2.02	$5.23e-04$	1.91	$6.60e-05$	2.55	$2.40e-03$	1.74
	3068	0.031	24700	$6.84e-04$	1.76	$1.17e-04$	1.93	$7.47e-06$	2.81	$6.89e-04$	1.61
	12579	0.015	100940	$1.67e-04$	1.99	$2.89e-05$	1.98	$9.24e-07$	2.96	$1.78e-04$	1.91
	50877	0.007	4076400	$4.12e-05$	2.00	$7.20e-06$	1.99	$1.29e-07$	2.81	$4.29e-05$	2.03
2	146	0.131	2466	$2.74e-04$	–	$6.18e-05$	–	$1.59e-05$	–	$5.59e-04$	–
	654	0.065	10917	$3.16e-05$	2.88	$1.23e-05$	2.14	$2.66e-06$	2.38	$9.84e-05$	2.31
	3068	0.031	50856	$2.83e-06$	3.12	$5.62e-07$	4.00	$6.59e-08$	4.78	$1.09e-05$	2.83
	12579	0.015	208020	$3.40e-07$	3.00	$6.31e-08$	3.10	$2.96e-09$	4.39	$1.36e-06$	2.95
	50877	0.007	840400	$4.20e-08$	2.99	$7.67e-09$	3.01	$2.00e-10$	3.85	$1.66e-07$	3.01
3	146	0.131	4164	$4.76e-06$	–	$1.58e-06$	4.94	$6.26e-07$	–	$2.62e-05$	–
	654	0.065	18480	$4.73e-07$	3.07	$2.78e-07$	2.31	$6.11e-08$	3.10	$3.00e-06$	2.89
	3068	0.031	86216	$9.83e-09$	5.01	$4.52e-09$	5.33	$6.07e-10$	5.96	$1.40e-07$	3.96
	12579	0.015	352830	$5.27e-10$	4.14	$1.66e-10$	4.67	$1.42e-11$	5.32	$8.00e-09$	4.06
	50877	0.007	1425800	$3.15e-11$	4.03	$8.91e-12$	4.19	$4.87e-13$	4.82	$5.05e-10$	3.95

Table 2: History of convergence of the approximation in Example 2.

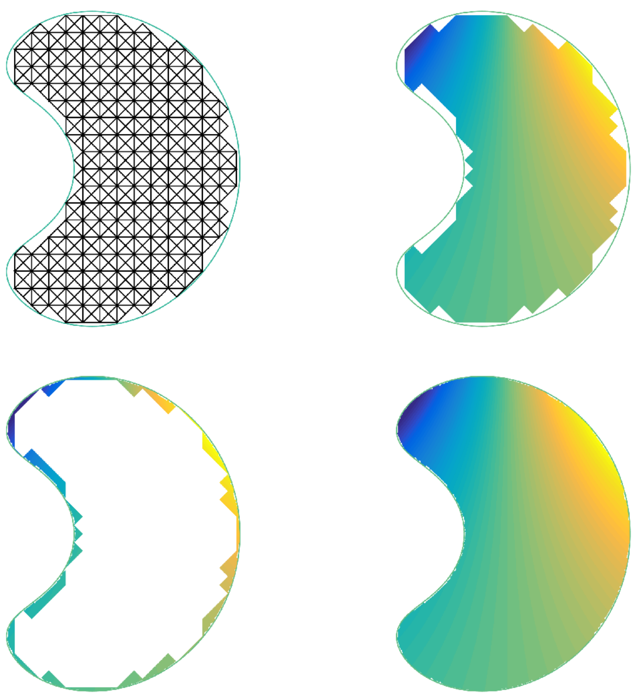

Figure 6: Example 2: $\sigma_{h,2}$ for the approximation $\mathbf{RT}_3 - \mathrm{P}_3$ with $N = 654$ elements.

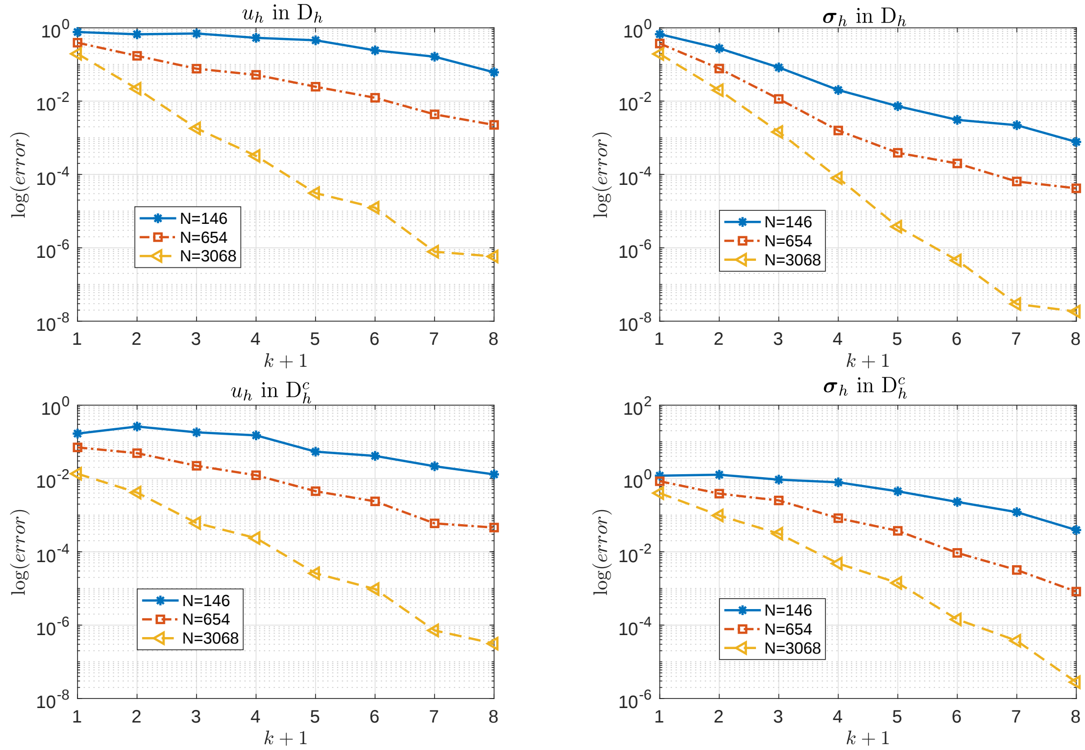

Figure 7: Example 3: Log of the *error* vs. $(k+1)$ for $k=\overline{0,7}$ and three fixed meshes.

2 and 0.5, respectively. In this case, the computational boundary Γ_h is defined through a piecewise linear interpolation of Γ as Figure 8 shows. Here, the distance $\mathrm{d}(\Gamma,\Gamma_h)$ is at most $\mathcal{O}(h^2)$. Table 3 shows that the experimental rates of convergence for $\mathtt{e_{int}}(\boldsymbol{\sigma})$, $\mathtt{e_{ext}}(\boldsymbol{\sigma})$ and $\mathtt{e_{int}}(u)$ are optimal, i.e., $\mathcal{O}(h^{k+1})$. In addition, the convergence rate of $\mathtt{e_{ext}}(u)$ is $\mathcal{O}(h^{k+3})$. This behavior can be explained by the proof of Theorem 3.7. In fact, since now $\widetilde{r}_e$ is of order h, the estimate becomes

$$\|u-u_h\|_{0,\mathrm{D}_h^c} \lesssim h^2\|\boldsymbol{\sigma}-\mathbf{E}_h(\boldsymbol{\sigma}_h)\|_{\mathrm{div}\,;\widetilde{\mathrm{T}}_h} \lesssim h^{k+3}.$$

Appendices

In this section we use the equivalence of the the norms $|||\cdot|||_e$ and $\|\cdot\|_{0,\widetilde{K}^e_{ext}}$ (cf. Lemma 3.4) to provide an estimate of $\widetilde{C}^e_{ext}$ defined in (2.14).

A Estimates of $\widetilde{C}^e_{ext}$

The following result extends the estimation in [17, Lemma A.1] to the case when the norm $\|\cdot\|_{0,\widetilde{K}^e_{ext}}$ is considered.

Lemma A.1. *Let e be any edge in $\mathcal{E}_h^\partial$. Let $\mathcal{L}$ be the line segment with endpoints given by the center of the biggest ball contained in K^e, and the point of the set $\widetilde{K}_{ext}$ where the polynomial p achieves its*

				Errors on D_h				Errors on D_h^c			
k	N	h	d.o.f	$\mathtt{e_{int}}(u)$	$\mathtt{r_{int}}(u)$	$\mathtt{e_{int}}(\boldsymbol{\sigma})$	$\mathtt{r_{int}}(\boldsymbol{\sigma})$	$\mathtt{e_{ext}}(u)$	$\mathtt{r_{ext}}(u)$	$\mathtt{e_{ext}}(\boldsymbol{\sigma})$	$\mathtt{r_{ext}}(\boldsymbol{\sigma})$
	150	0.660	395	$1.39e-01$	–	$1.26e-01$	–	$8.03e-05$	–	$9.38e-02$	–
	608	0.355	1560	$6.89e-02$	1.00	$6.25e-02$	1.00	$9.51e-06$	3.04	$4.62e-02$	1.01
0	2396	0.187	6070	$3.50e-02$	0.98	$3.16e-02$	0.99	$1.16e-06$	3.05	$2.35e-02$	0.98
	9358	0.095	23555	$1.78e-02$	0.99	$1.61e-02$	0.99	$1.46e-07$	3.04	$1.18e-02$	1.00
	37798	0.050	94815	$8.98e-03$	0.98	$8.05e-03$	0.99	$1.87e-08$	2.94	$5.99e-03$	0.97
	150	0.660	1240	$8.68e-03$	–	$1.10e-02$	–	$2.42e-05$	–	$1.39e-02$	–
	608	0.355	4944	$2.23e-03$	1.93	$2.73e-03$	1.99	$1.68e-06$	3.81	$3.36e-03$	2.03
1	2396	0.187	19328	$5.69e-04$	1.99	$6.98e-04$	1.99	$1.02e-07$	4.07	$9.36e-04$	1.86
	9358	0.095	75184	$1.46e-04$	1.98	$1.79e-04$	1.99	$7.27e-09$	3.89	$2.44e-04$	1.97
	37798	0.050	30302	$3.63e-05$	2.00	$4.44e-05$	1.99	$4.72e-10$	3.91	$6.31e-05$	1.94
	150	0.660	2535	$5.86e-04$	–	$5.65e-04$	–	$1.44e-06$	–	$6.96e-04$	–
	608	0.355	10152	$6.99e-05$	3.03	$7.02e-05$	2.98	$5.43e-08$	4.68	$1.01e-04$	2.74
2	2396	0.187	39774	$8.92e-06$	3.00	$9.17e-06$	2.96	$1.70e-09$	5.04	$1.40e-05$	2.88
	9358	0.095	154890	$1.14e-06$	3.01	$1.18e-06$	2.99	$5.64e-11$	5.00	$1.73e-06$	3.06
	37798	0.050	624630	$1.42e-07$	2.98	$1.47e-07$	2.99	$1.90e-12$	4.85	$2.40e-07$	2.83
	150	0.660	4280	$1.81e-05$	–	$2.36e-05$	–	$6.37e-08$	–	$4.11e-05$	–
	608	0.355	17184	$1.29e-06$	3.77	$1.49e-06$	3.94	$8.55e-10$	6.16	$2.80e-06$	3.84
3	2396	0.187	67408	$8.32e-08$	4.00	$9.66e-08$	3.99	$1.58e-11$	5.81	$1.78e-07$	4.01
	9358	0.095	262660	$5.54e-09$	3.97	$6.37e-09$	3.99	$2.55e-13$	6.05	$1.21e-08$	3.93
	37798	0.050	1059600	$3.38e-10$	4.00	$3.90e-10$	3.99	$4.13e-15$	5.90	$8.40e-10$	3.83

Table 3: History of convergence of the approximation in Example 4.

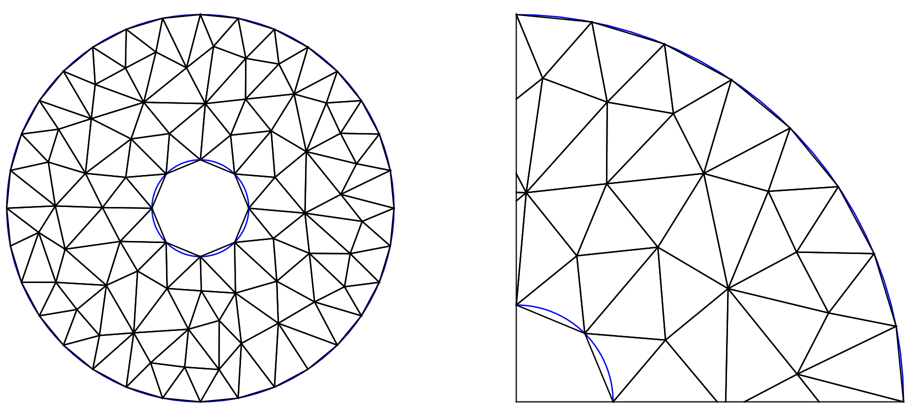

Figure 8: Example 4: (Left) Mesh with $N = 150$ elements, where Γ_h is constructed by piecewise linear interpolation of the boundary Γ (blue line). (Right) Part of the domain Ω that lies in the first quadrant of the Cartesian plane.

maximum. Suppose that assumption (A.1) *holds. Assume further that $\mathcal{L}$ is contained in interior of the closure of the set $K^e \cup \widetilde{K}^e_{ext}$, denoted by B^e. Then, for any $p \in \mathrm{P}_l(B^e)$ we have*

$$\|p\|_{0,\widetilde{K}^e_{ext}} \leq C(\widetilde{r}_e)^{1/2}(l+1)^2\eta_e^l\|p\|_{0,K^e},$$

where $\widetilde{r}_e := \widetilde{H}_e/h_e^{\perp}$ and $\eta_e := 1+2\gamma_{K^e}\widetilde{r}_e+2\Big(\gamma_{K^e}\widetilde{r}_e(1+\gamma_{K^e}\widetilde{r}_e)\Big)^{1/2}$. Here the constant C solely depends on the shape-regularity constant γ_{K^e}.

Proof. We begin by noting that $\mathcal{L}$ can be subdivided as

$$I^e_{int} := \Big\{\mathbf{x} \in \mathcal{L} :\ \mathbf{x} \cap K^e \neq \varnothing\Big\} \quad \text{and} \quad I^e_{ext} := \Big\{\mathbf{x} \in \mathcal{L} :\ \mathbf{x} \cap \widetilde{K}^e_{ext} \neq \varnothing\Big\},$$

from which

$$\|p\|^2_{0,\widetilde{K}^e_{ext}} \leq |\widetilde{K}^e_{ext}| \max_{\mathbf{x}\in\widetilde{K}^e_{ext}} |p(\mathbf{x})| \leq |\widetilde{K}^e_{ext}| \|p\|^2_{\mathrm{L}^\infty(I^e_{ext})} \leq C h^{d-1}_{K^e} \|p\|^2_{\mathrm{L}^\infty(I^e_{ext})},$$

owing to the relation $|\widetilde{K}^e_{ext}| \leq C h^{d-1}_{K^e}$. Next, we proceed as in [17, Lemma A.1] and prove that $\|p\|_{\mathrm{L}^\infty(I^e_{ext})} \leq \eta^l_e \|p\|_{\mathrm{L}^\infty(I^e_{int})}$. In fact, in virtue of [13, Lemma 4.3], this is fulfilled by observing that

$$\frac{|I^e_{ext}|}{|I^e_{int}|} \leq \frac{|I^e_{ext}|}{\rho_{K^e}} \leq \frac{\widetilde{H}_e}{\rho_{K^e}} \leq \gamma_{K^e} \frac{\widetilde{H}_e}{h_{K^e}} \leq \gamma_{K^e} \widetilde{r}_e,$$

where ρ_{K^e} is the radius of the biggest ball contained in K^e, since $h^\perp_e \leq h_{K^e}$ and $h_{K^e} \leq \gamma_{K^e}\rho_{K^e}$. In addition, by standard scaling arguments there holds

$$\|p\|_{\mathrm{L}^\infty(I^e_{int})} \leq \|p\|_{\mathrm{L}^\infty(K^e)} \leq C\,(h_{K^e})^{-\frac{d}{2}}\,(l+1)^2 \|p\|_{0,K^e}.$$

Finally, the proof is completed by noting that $h^{-1}_{K^e} \leq \left(h^\perp_e\right)^{-1} \leq \widetilde{r}_e / \widetilde{H}_e$. ∎

The previous result, together with the estimates in Lemma 3.4, implies that

$$\widetilde{C}^e_{ext} \leq (C^e_1)^{-1} C^e_2 (l+1)^2 \eta^l_e.$$

6 Concluding remarks

We have proposed and analyzed a mixed finite element method for diffusive problems with Dirichlet boundary condition on a curved domain Ω with boundary Γ. In particular, we have considered a novel technique in which the approximation to the solution is first computed over a polygonal subdomain D_h of Ω and then extended to the complement $\mathrm{D}^c_h = \Omega \setminus \overline{\mathrm{D}_h}$ of D_h. We showed that our $\mathbf{H}(\mathrm{div}\,;\mathrm{D}_h)$-conforming method, is well-posed and optimal provided the approximation of the boundary data given in (2.8). We presented numerical experiments validating our theory.

On the other hand, as Remark 3.1 mentioned, we observe that our analysis is independent of how the computational subdomain D_h and the *transferring paths* are constructed, as long as Assumptions **A**, **D** and assumptions of Lemma 3.4 are satisfied. Moreover, as it is mentioned in Remark 3.2, our technique also covers the case of a fitted method resulting of interpolating the boundary Γ by a piecewise linear function. Finally, we believe the theory developed in this work can be adapted to three dimensions. In fact, the result in Theorem 2.2 and the estimates in Section 3.1 are independent of the dimension of the problem.

References

[1] S. Beuchler, V. Pillwein and S. Zaglmayr, *Sparsity optimized high order finite element functions for H(div) on simplices.* Numer. Math. 122 (2012), no. 2, 197–225.

[2] D.P. Bertsekas, *Convex Analysis and Optimization.* Athena Scientific, Belmont, Mass, 2003.

[3] J.H. Bramble, T. Dupont V. and Thomée. *Projection methods for Dirichlet's problem in Approximating polygonal domains with boundary-value corrections.* Math. Comp., 26 (1994), no 120, 869–879.

[4] J.H. Bramble and J.T. King, *A robust finite element method for nonhomogeneous Dirichlet problems in domains with curved boundaries.* Math. Comp. 63 (1994), 1–17.

[5] J.H. Bramble and J.T. King, *A finite element method for interface problems in domains with smooth boundaries and interfaces.* Advances in Comp. Math. 6 (1996), 109–138.

[6] S.C. Brenner and L.R. Scott, *The mathematical theory of finite element methods.* Third edition. Texts in Applied Mathematics, 15. Springer, New York, 2008.

[7] F. Bertrand and G. Starke, *Parametric Raviart-Thomas elements for mixed methods on domains with curved surfaces.* SIAM J. Numer. Anal. 54 (2016), no. 6, 3648–3667.

[8] F. Bertrand, S. Müzenmaier, and G. Starke, *First-order system least squares on curved boundaries: Higher-order Raviart–Thomas elements.* SIAM J. Numer. Anal., 52 (2014), pp. 3165–3180.

[9] F. Brezzi and M. Fortin, *Mixed and hybrid finite element methods.* Springer Series in Computational Mathematics, 15. Springer-Verlag, New York, 1991.

[10] P.G. Ciarlet, *The finite element method for elliptic problems.* Studies in Mathematics and its Applications, Vol. 4. North-Holland Publishing Co., Amsterdam-New York-Oxford, 1978.

[11] E. Colmenares, G. N. Gatica, R. Oyarzua. *Analysis of an augmented mixed-primal formulation for the stationary Boussinesq problem.* Numer. Methods Partial Differ. Equ. 32 (2016), no. 2, 445–478.

[12] D.A. Di Pietro and A. Ern, *Mathematical aspects of discontinuous Galerkin methods.* Mathématiques & Applications (Berlin) [Mathematics & Applications], 69. Springer, Heidelberg, 2012.

[13] B. Cockburn, D. Gupta and F. Reitich, *Boundary-conforming discontinuous Galerkin methods via extensions from subdomains.* J. Sci. Comput. 42 (2010), no. 1, 144–184.

[14] B. Cockburn, F.-J Sayas and M. Solano, *Coupling at a distance HDG and BEM.* SIAM J. Sci. Comput. 34 (2012), no. 1, A2–A47.

[15] B. Cockburn and M. Solano, *Solving Dirichlet boundary-value problems on curved domains by extensions from subdomains.* SIAM J. Sci. Comput. 34 (2012), no. 1, A497–A519.

[16] B. Cockburn and M. Solano, *Solving convection-diffusion problems on curved domains by extensions from subdomains.* J. Sci. Comput. 59 (2014), no. 2, 512–543.

[17] B. Cockburn, W. Qiu and M. Solano, *A priori error analysis for HDG methods using extensions from subdomains to achieve boundary conformity.* Math. Comp. 83 (2014), no. 286, 665–699.

[18] B. Cockburn and W. Zhang, *A posteriori error estimates for HDG methods.* J. Sci. Comput. 51 (2012), no. 3, 582–607.

[19] T.A. Davis, *Algorithm 832: UMFPACK V4.3 - an unsymmetric-pattern multifrontal method.* ACM Transactions on Mathematical Software, vol. 30, pp. 196-199, (2004).

[20] S. Deng and W. Cai, *Analysis and application of an orthogonal nodal basis on triangles for discontinuous spectral element methods*. Appl. Numer. Anal. Comput. Math. 2 (2005), no. 3, 326–345.

[21] G.N. Gatica, *A Simple Introduction to the Mixed Finite Element Method. Theory and Applications*. Springer Briefs in Mathematics, Springer, Cham, 2014.

[22] G.N. Gatica, R. Ruiz–Baier and G. Tierra *A mixed finite element method for Darcy s equations with pressure dependent porosity*. Math. Comp. 85 (2016), no. 297, 1–33.

[23] V. Girault and P.-A. Raviart, *Finite element approximation of the Navier-Stokes equations*. Lecture Notes in Mathematics, 749. Springer-Verlag, Berlin-New York, 1979.

[24] R. Hiptmair, *Finite elements in computational electromagnetism*. Acta Numer. 11 (2002), 237–339.

[25] M. Lenoir, *Optimal isoparametric finite elements and errors estimates for domains involving curved boundaries*. SIAM J. Numer. Anal. 23 (1986), 562–580.

[26] R.J. LeVeque and Z. Li. *Immersed interface methods for Stokes flow with elastic boundaries or surface tension*. SIAM J. Sic. Comput. 18 (1997), no 3, 709–735.

[27] Y. Mori, *Convergence proof of the velocity field for a Stokes flow immersed boundary method*. Comm. Pure and Appl. Math., 160 (2008), 1213–1263.

[28] C.S. Peskin, *Flow patterns around heart valves: a numerical method*. J. Comput. Phys., 10 (1972), 252–271.

[29] W. Qiu, M. Solano and P. Vega, *A High Order HDG Method for Curved-Interface Problems Via Approximations from Straight Triangulations*. J. Sci. Comput. 69 (2016), no. 3, 1384–1407.

[30] J.E. Roberts and J.-M. Thomas, *Mixed and hybrid methods*. Handbook of numerical analysis, Vol. II, 523–639, Handb. Numer. Anal., II, North-Holland, Amsterdam, 1991.

[31] M. Solano and F. Vargas, *A high order HDG method for Stokes flow in curved domains*. Submitted.

[32] E.M. Stein, *Singular integrals and differentiability properties of functions*. Princeton Mathematical Series, No. 30 Princeton University Press, Princeton, N.J. 1970.